山东大学
SHANDONG UNIVERSITY

第一届长三角海洋机器人国际研讨会

水下智能感知与理解

UNDERWATER INTELLIGENT PERCEPTION & UNDERSTANDING

报告人：丛润民

山东大学控制科学与工程学院

机器智能与系统控制教育部重点实验室

—— 学无止境 气有浩然 ——

Outline

- Introduction
- Technical Methods
  - PUGAN: Physical Model-guided Underwater Image Enhancement Using GAN With Dual-Discriminators (TIP’23)
  - WaterMask: Instance Segmentation For Underwater Imagery (ICCV’23)
  - Diving Into Underwater: Segment Anything Model Guided Underwater Salient Instance Segmentation And A Large-scale Dataset (ICML’24)
- Future work

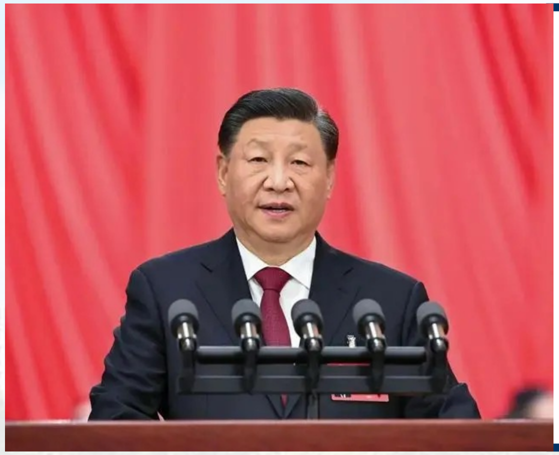

习近平总书记在二十大报告中指出——

（四）促进区域协调发展。发展海洋经济，保护海洋生态环境，加快建设海洋强国。

中华人民共和国中央人民政府

《中华人民共和国国民经济和社会发展第十四个五年规划和2035年远景目标纲要》

积极拓展海洋经济发展空间。聚焦新一代信息技术、生物技术、新能源、新材料、高端装备、新能源汽车、绿色环保以及航空航天、海洋装备等战略性新兴产业，加快关键核心技术创新应用，增强要素保障能力，培育壮大产业发展新动能。深化军民科技协同创新，加强海洋、空天、网络空间、生物、新能源、人工智能、量子科技等领域军民统筹发展，推动军地科研设施资源共享，推进军地科研成果双向转化应用和重点产业发展。

智慧海洋工程是全面提升经略海洋能力的整体解决方案。

Introduction

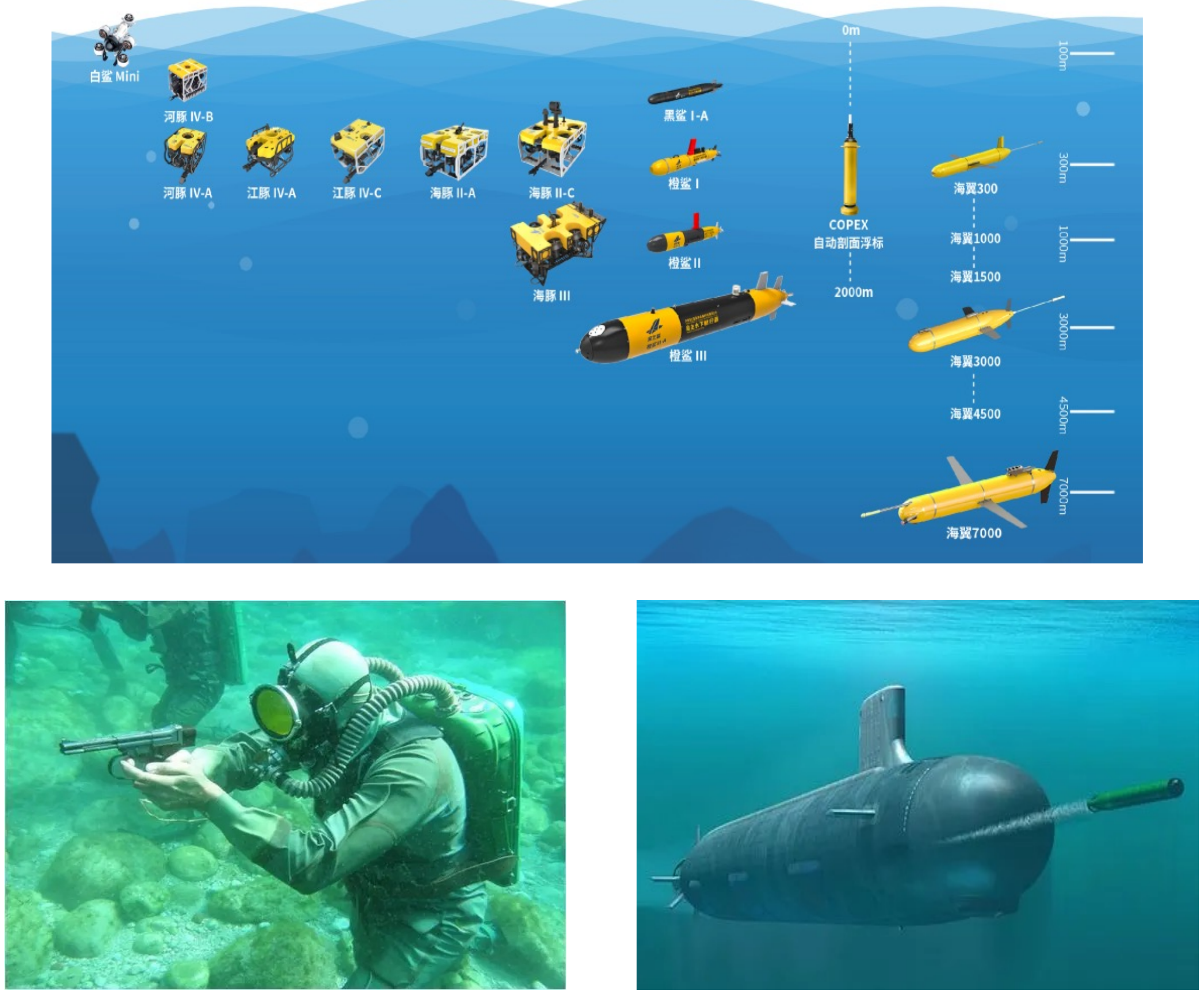

Equipment

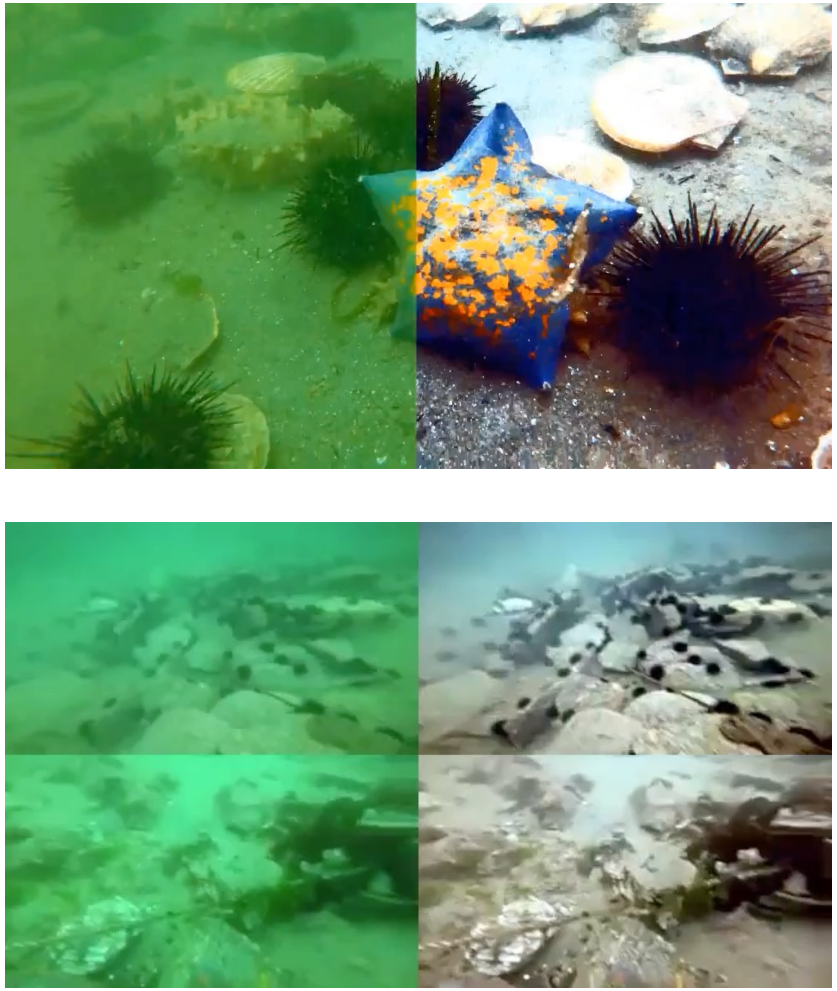

Underwater imaging

水下内容感知增强

Underwater Content Perception & Enhancement

Underwater Image Enhancement

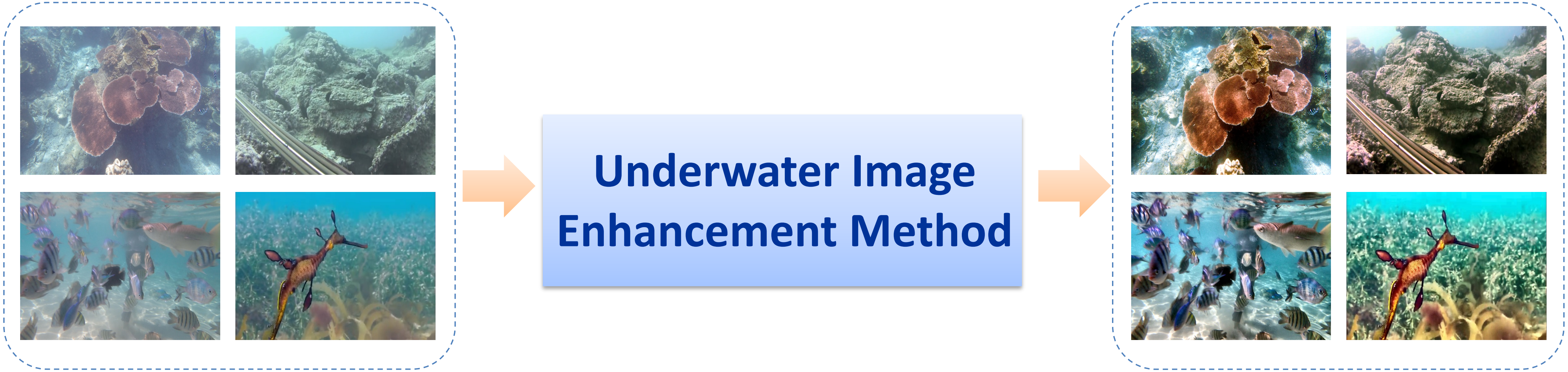

Underwater Image Enhancement Method

Inputs:
Underwater images

Outputs:
Enhanced Underwater images

Underwater image enhancement methods improve the visibility of underwater images, eliminate color deviation and stretch contrast, and effectively improve the visual quality of images.

Top 50 Popular Documents in IEEE TIP

PUGAN: Physical Model-Guided Underwater Image Enhancement Using GAN with Dual-Discriminators

Runmin Cong, Wenyu Yang, Wei Zhang, Chongyi Li, Chun-Le Guo, Qingming Huang, and Sam Kwong

***IEEE Transactions on Image Processing*, 2023**

https://rmcong.github.io/proj_PUGAN.html

Traditional method

Non physical model method

Some of these methods directly apply existing image enhancement methods to underwater image data, and there are also specialized algorithms designed specifically for the characteristics of underwater images.

Physical models-based method

Mathematical modeling of the degradation process of underwater images, parameter estimation based on the model, and then inversion to obtain clear underwater images.

Traditional method

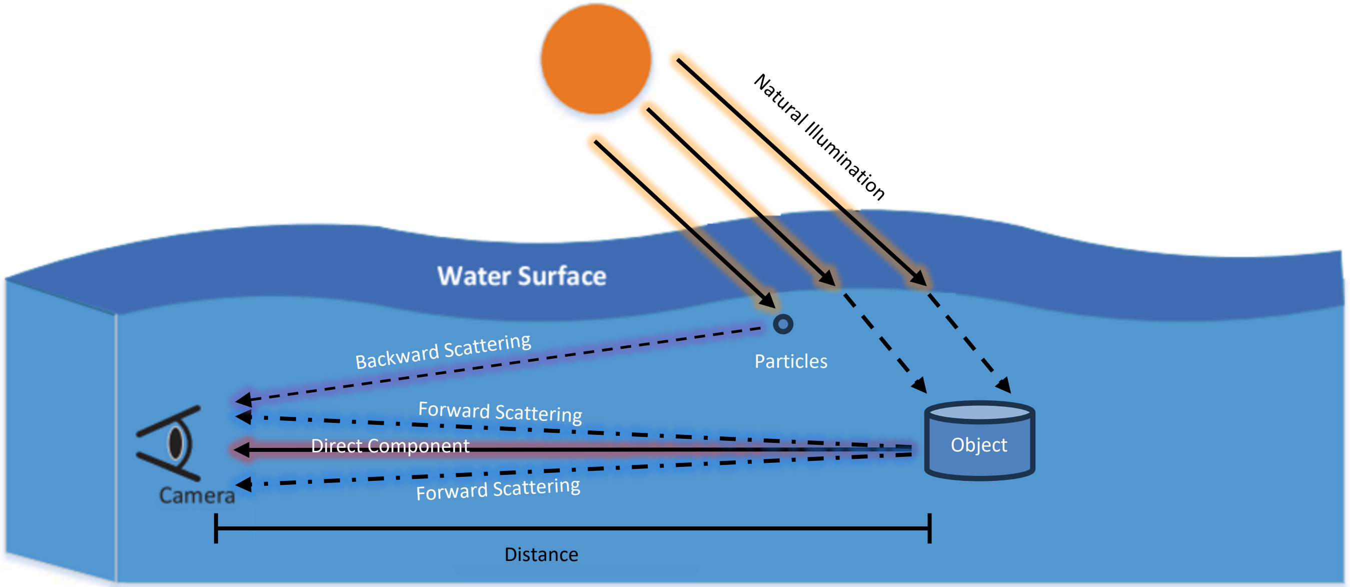

$$I(x) = J(x)t(x) + A(1 - t(x))$$

where I is the observed underwater image, J denotes the restored image, A represents the background light, and t is the transmission map, describing the portion of the light that is not scattered and reaches the camera.

Motivation

- Traditional methods based on **non-physical models largely rely on handmade feature design**, which makes them prone to over or under enhancement, thereby affecting the overall visual effect. Although modeling the underwater imaging process is beneficial for solving the unique visual problems of underwater images, **relying solely on physical models is not reliable because it is difficult to simulate a universal model to cope with complex underwater environments**.
- The deep learning method utilizes the powerful learning ability of deep networks and can achieve good results in certain situations. However, underwater environments are often complex and diverse, and **relying solely on network learning may distort the enhanced results**.

Therefore, we hope to design a network architecture that can effectively combine them to play to complementary advantages and collaborative promotion.

Contributions

- Considering the respective advantages of the physical model and the GAN model for the UIE task, we propose a **Physical Model-Guided framework using GAN with Dual-Discriminators (PUGAN)**, consisting of a Phy-G and a Dual-D. Extensive experiments on three benchmark datasets demonstrate that our PUGAN outperforms state-of-the-art methods in both qualitative and quantitative metrics.
- We design **two subnetworks in the Phy-G**, including the **Par-subnet** and the **TSIE-subnet**, for the parameter estimation of physical model and the physical model guided CNN-based enhancement, respectively. On the one hand, we introduce an intermediate variable in the Par-subnet, i.e., depth, to enable effective estimation of the transmission map. On the other hand, we propose a **DQ module in TSIE-subnet** to quantify the distortion degrees and achieve targeted encoder feature reinforcing.
- In addition to the pixel-level global similarly loss and perceptual loss, we design **the style-content adversarial loss in the Dual-D** to constrain the style and content of the enhanced underwater image to be realistic.

Our Method

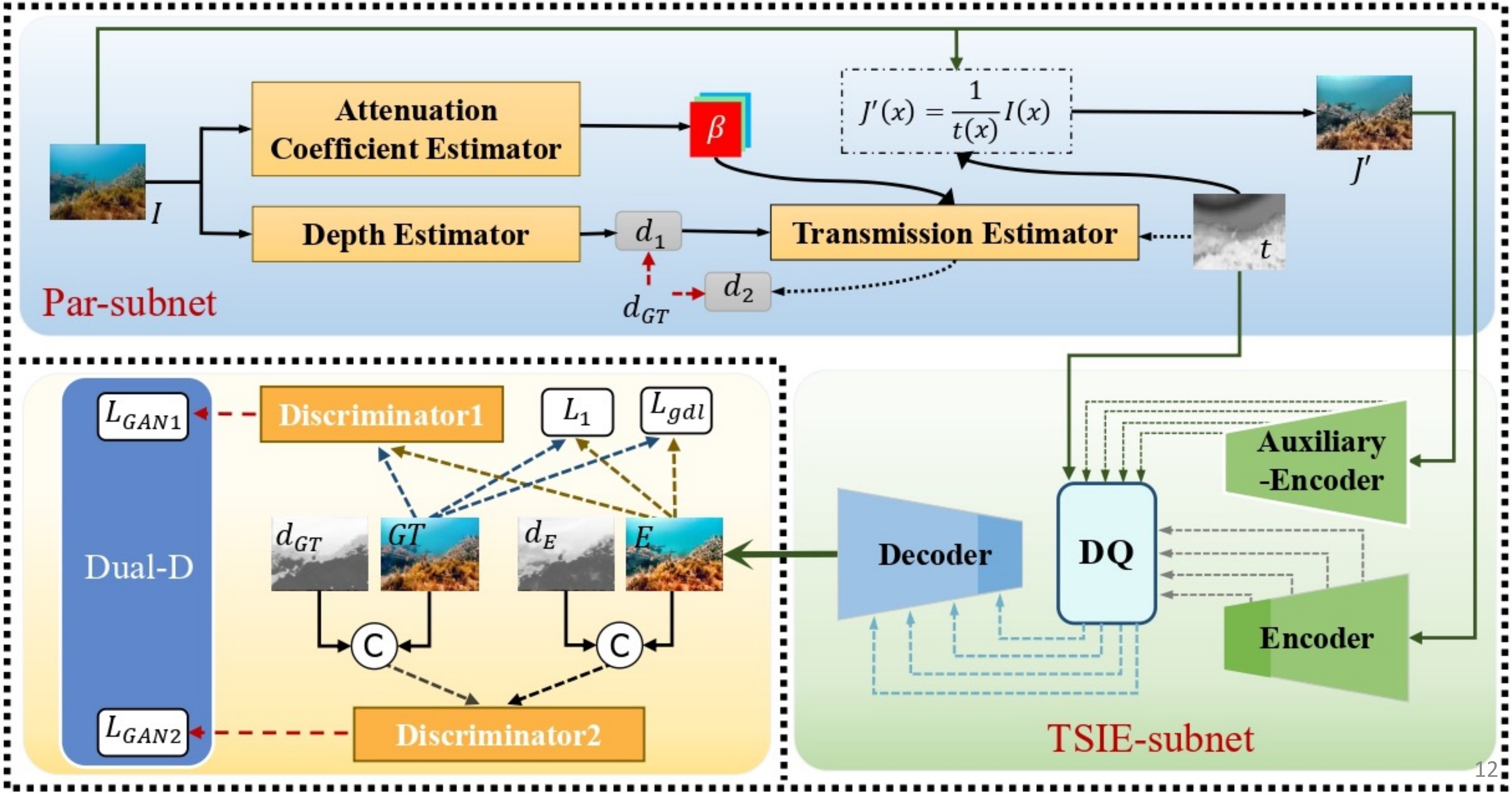
Attenuation Coefficient Estimator
β
$J'(x) = \frac{1}{t(x)} I(x)$
J'
I
Depth Estimator
d_1
Transmission Estimator
t
d_{GT}
d_2
Par-subnet
L_{GAN1}
Discriminator1
L_1
L_{gdl}
Dual-D
d_{GT}
GT
d_E
E
C
C
L_{GAN2}
Discriminator2
Decoder
DQ
Auxiliary -Encoder
Encoder
TSIE-subnet

Par-subnet

The physical model of the underwater imaging process：

$$I(x) = J(x)t(x) + A(1 - t(x))$$

$$t(x) = e^{-\beta d(x)}$$

t is the transmission map, describing the portion of the light that is not scattered and reaches the camera, β is the attenuation coefficient of the water, and d is the depth of scene. Therefore, the depth can also reflect the attenuation of the scene to a certain extent.

We can inversely derive the calculation formula of the enhanced image J as:

$$J(x) = \frac{1}{t(x)} I(x) - A\left(\frac{1}{t(x)} - 1\right)$$

correct the color

remove the influence of background light

obtaining color-corrected underwater images through physical model inversion during the first stage

$$J'(x) = \frac{1}{t(x)} I(x)$$

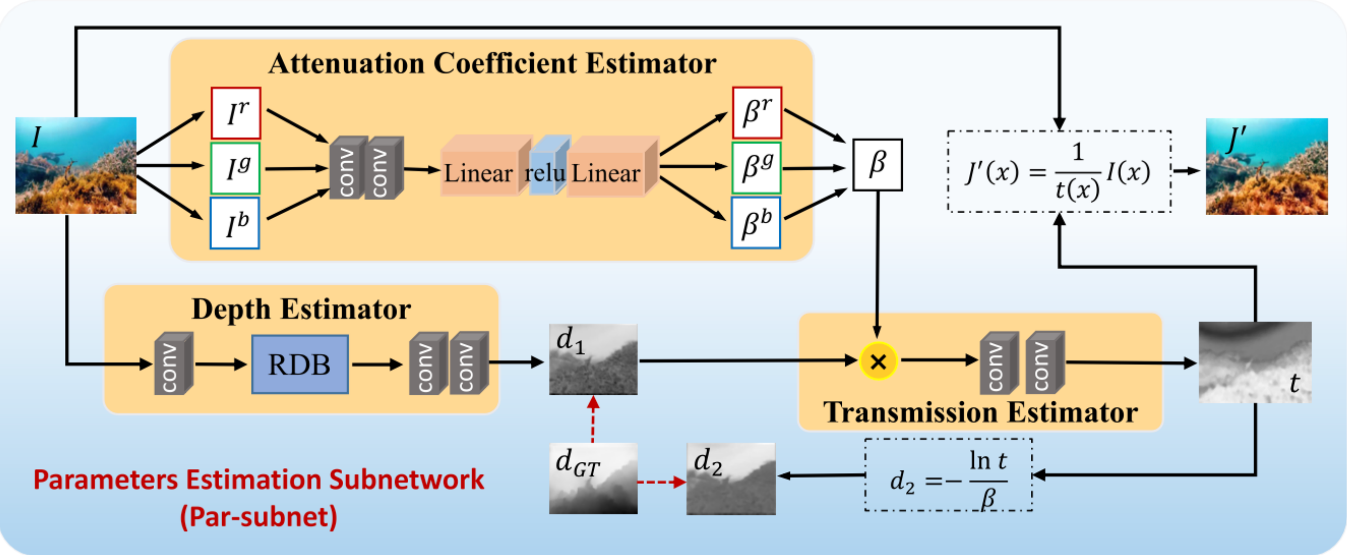

Parameters Estimation Subnetwork (Par-subnet)

$$\beta^c = linear(relu(linear(conv.p.r(I^c))))$$

$$\beta = cat(\beta^r, \beta^g, \beta^b)$$

$$d_1 = \sigma(conv(conv.b.r(\mathrm{RDB}(conv.b.r(I)))))$$

$$t = \sigma(conv(conv.b.r(d_1 \cdot \beta)))$$

$$d_2 = -\frac{\ln t}{\beta}$$

TSIE-subnet

In the first stage, we invert color-enhanced underwater images with better interpretability using the learned physical model parameters. But as mentioned before, **the enhancement effect is not perfect due to the exclusion of background light**.

Therefore, we re-enhance the underwater images under the CNN network architecture in the second stage guided by the color-enhanced images, thereby forming a two-stream architecture to realize the interaction of multi-source information.

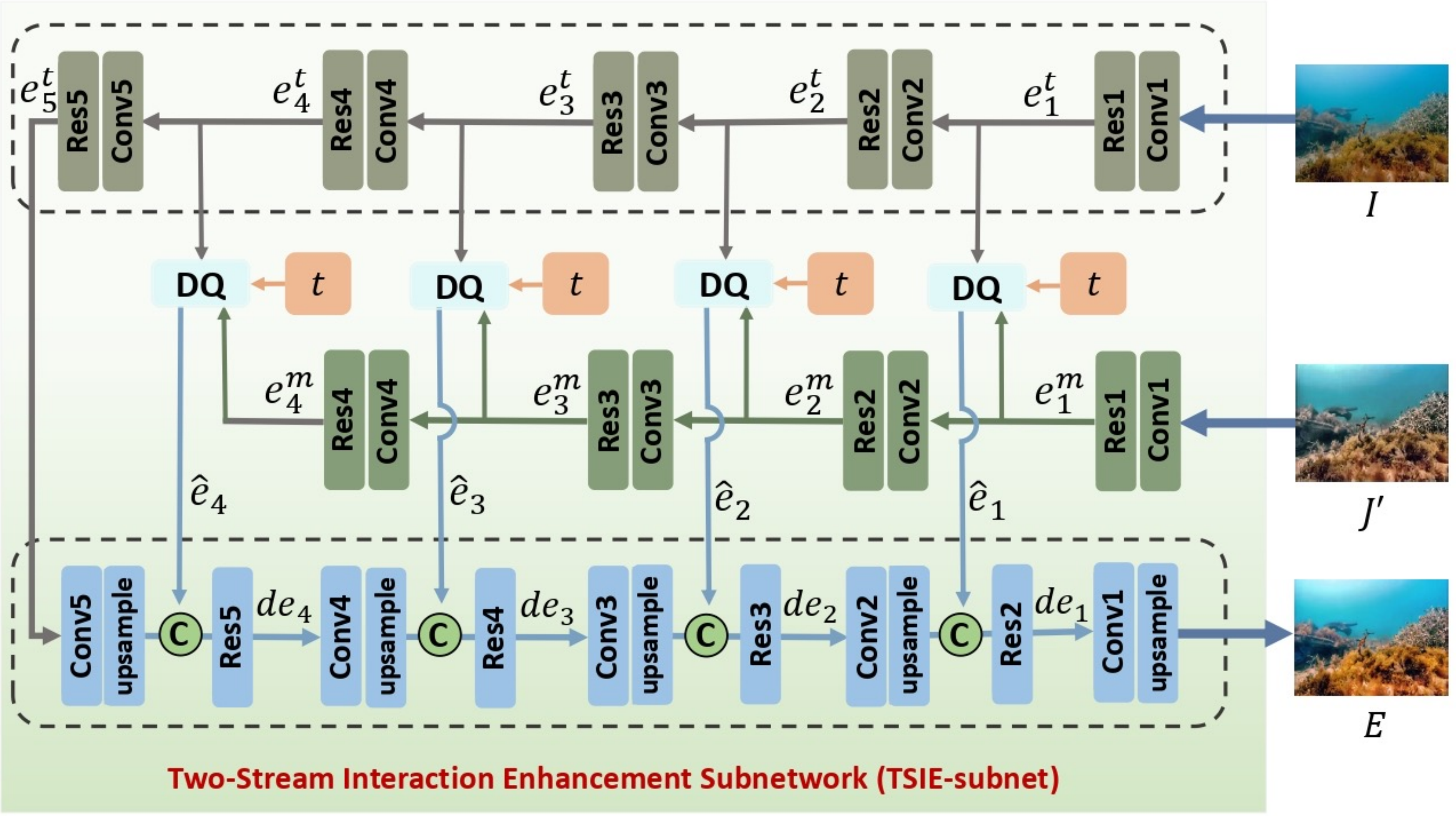

Two-Stream Interaction Enhancement Subnetwork (TSIE-subnet)

Degradation Quantization (DQ)

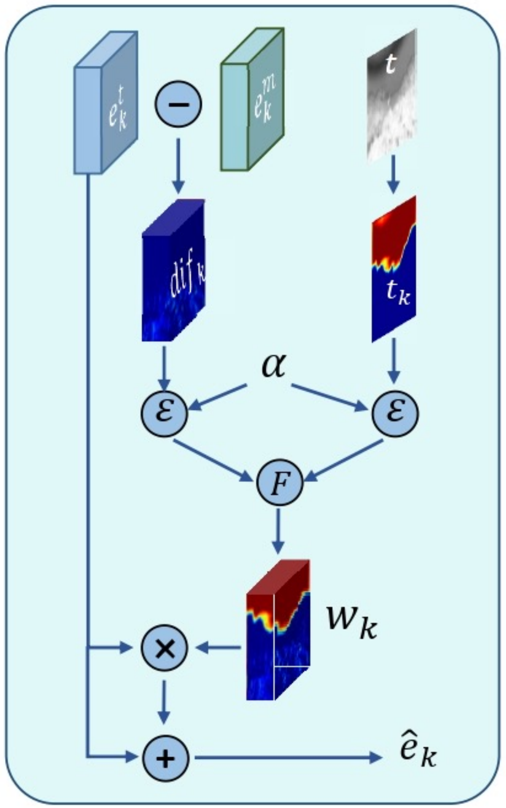

TSIE-subnet

Degradation Quantization (DQ)

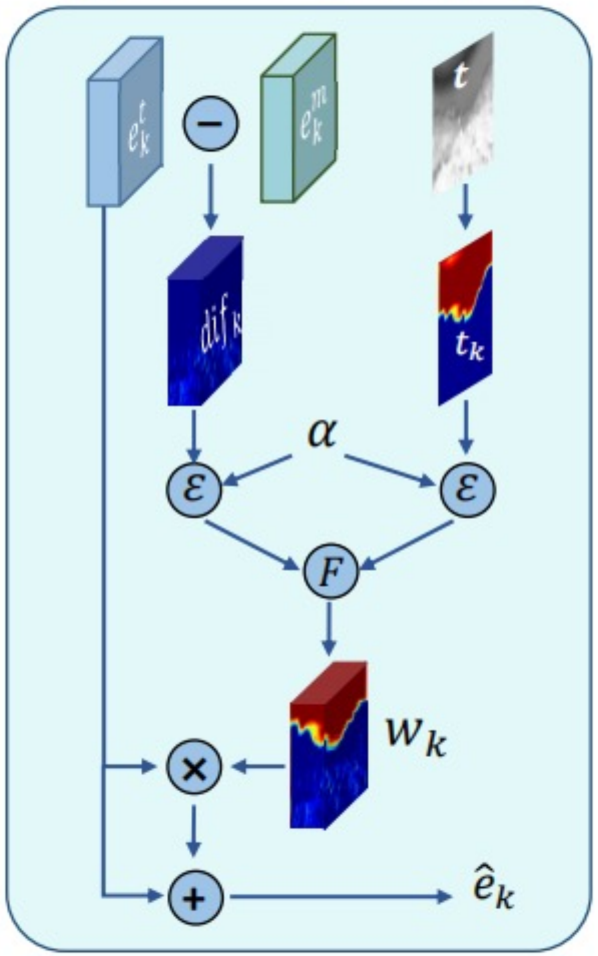

On the one hand, we can locate severely degraded regions by directly comparing the difference between the color enhanced image features and the original image features, which can be described as:

$$dif_k = conv.b.r(|e_k^t - e_k^m|) \cdot \varepsilon(conv.b.r(|e_k^t - e_k^m|) - \alpha)$$

On the other hand, the degree of degradation of underwater images is negatively correlated with the transmission characteristics. Therefore, we can also identify some regions that are prone to degradation from the transmission map:

$$t_k = (1 - maxpool(t)) \cdot \varepsilon(1 - maxpool(t) - \alpha)$$

Combining these two aspects, the final weights can be defined as follows：

$$w_k = \sigma(conv((conv.b.r(t_k + di\,f_k))))$$

Subsequently, these weights are applied to the input features e^k to generate the updated features $\hat{e}^k$ through the residual connection:

$$\hat{e}_k = e_k^t + e_k^t \otimes w_k$$

Loss Function

For Par-subnet:

We first train the attenuation coefficient estimator and then freeze their parameters to train the depth estimator and transmission estimator. To control the accuracy of the transmission map, we use the transmission map and attenuation coefficient to compute the depth map again. Therefore, the loss of Par-subnet is defined as follows:

$$L_p = \frac{1}{H \times W}[\sum_{m=1}^{H}\sum_{n=1}^{W}(|d(m,n) - d_1(m,n)|) + \sum_{m=1}^{H}\sum_{n=1}^{W}(|d(m,n) - d_2(m,n)|)] + \frac{1}{3}\sum_{c=1}^{3}(|\hat{\beta}^c - \beta^c|)$$

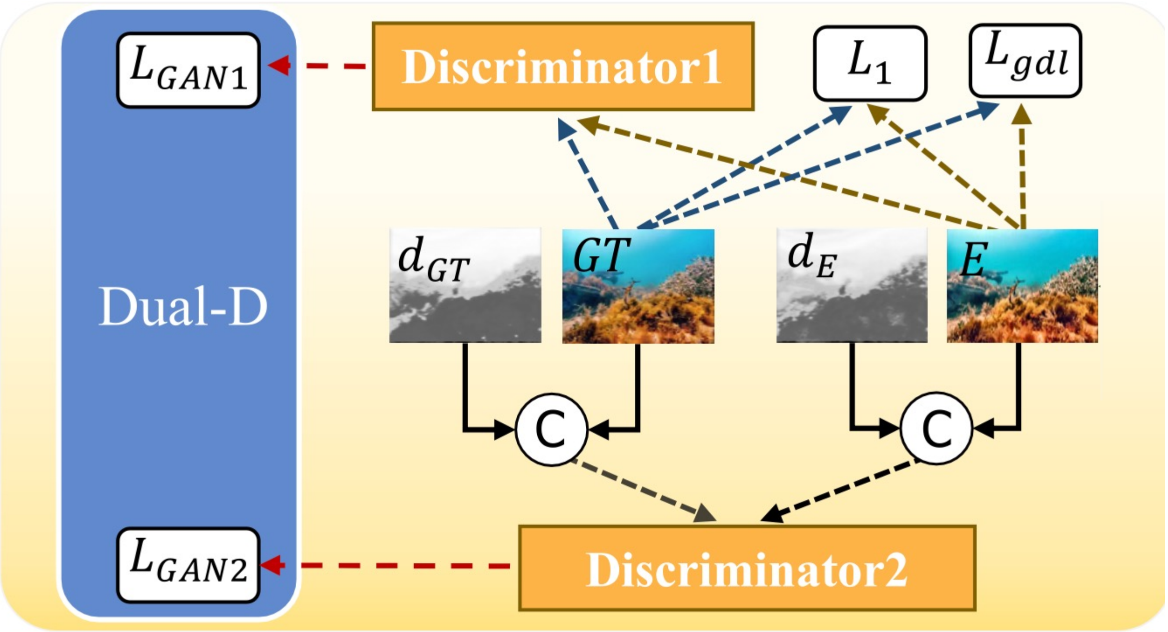

For Phy-G:

In order to make the generated image as visually pleasing as possible while maintaining its authenticity of the image, we use global similarly loss, perceptual loss and adversarial loss to compose the final loss:

$$L = \lambda_1 \cdot \arg\min_{G}\max_{D_1} L_{GAN1}(G, D_1) + \lambda_2 \cdot \arg\min_{G}\max_{D_2} L_{GAN2}(G, D_2) + \lambda_3 \cdot L_1(E, Y) + \lambda_4 \cdot L_{gdl}(E, Y)$$

$$\arg\min_{G}\max_{D_1} L_{GAN_1}(G, D_1) = \mathbb{E}_{\{I,Y\}}[\log D_1(Y)] + \mathrm{E}_{\{I,Y\}}[\log(1 - D_1(E))]$$

$$\arg\min_{G}\max_{D_2} L_{GAN_2}(G, D_2) = \mathbb{E}_{\{I,Y,d\}}[\log D_2(Y, d_Y)] + \mathbb{E}_{\{I,Y,d\}}[\log(1 - D_2(E, d_E))]$$

Experiments

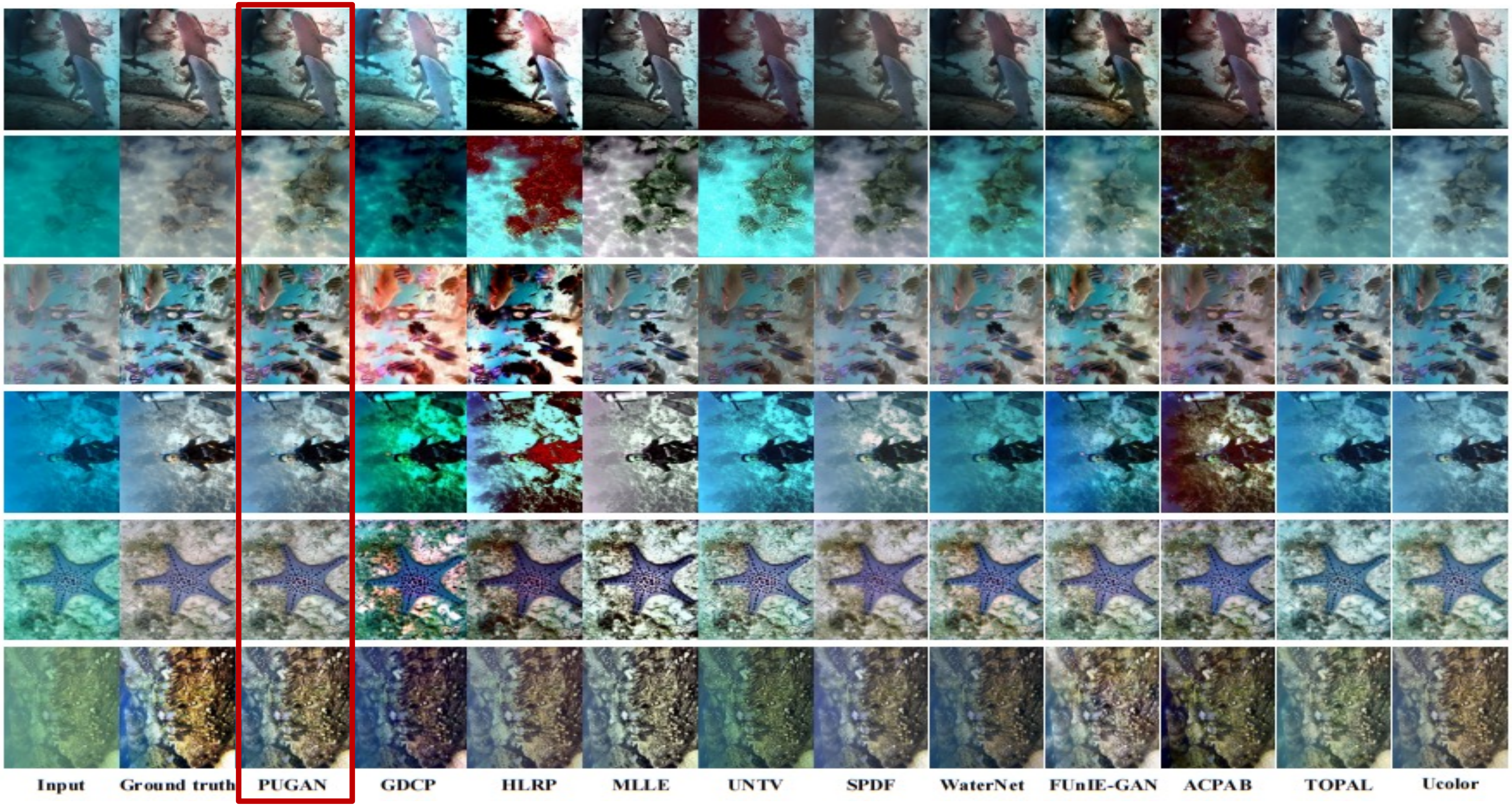

Experiments

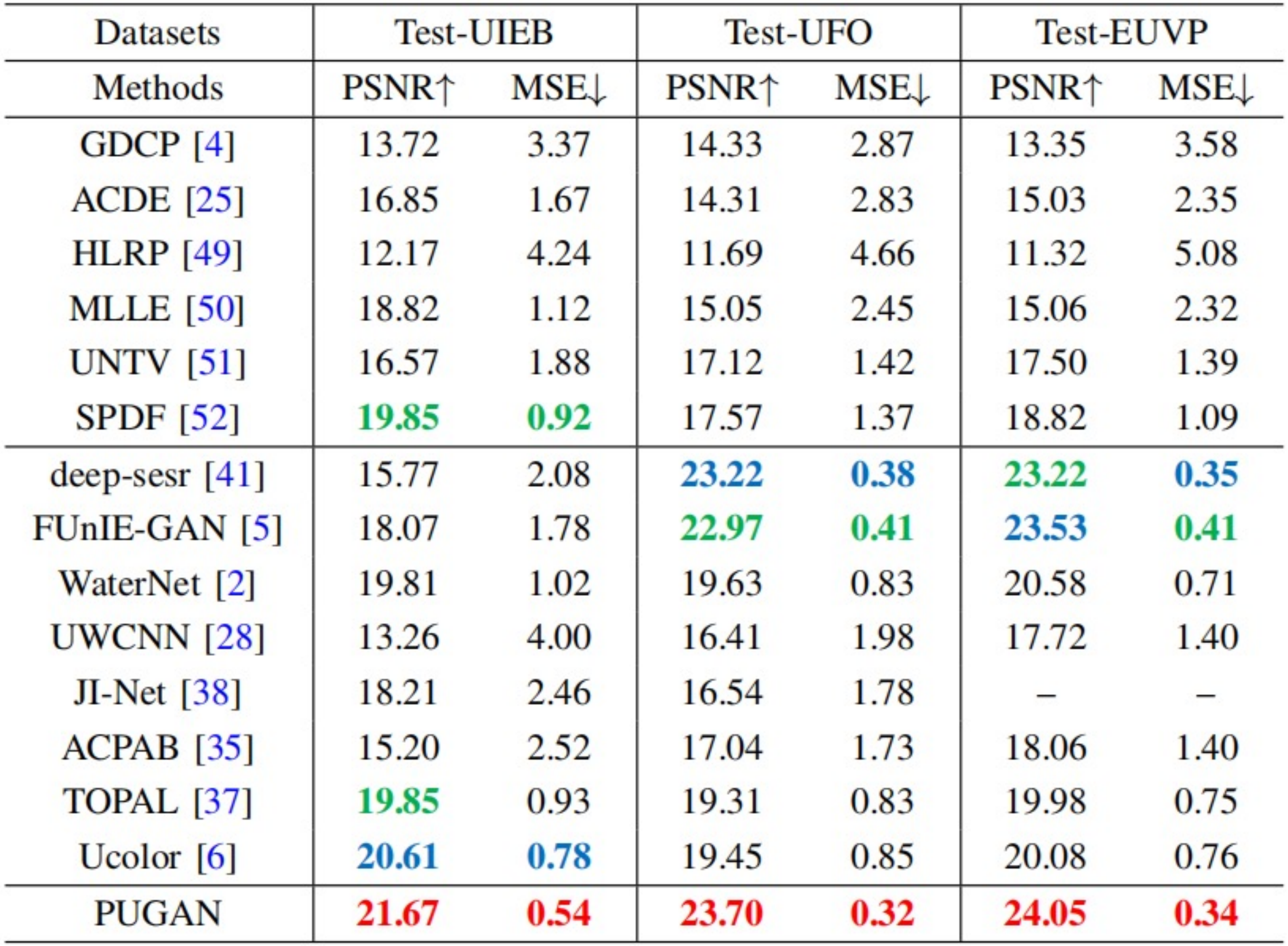

Datasets	Test-UIEB		Test-UFO		Test-EUVP	
Methods	PSNR↑	MSE↓	PSNR↑	MSE↓	PSNR↑	MSE↓
GDCP [4]	13.72	3.37	14.33	2.87	13.35	3.58
ACDE [25]	16.85	1.67	14.31	2.83	15.03	2.35
HLRP [49]	12.17	4.24	11.69	4.66	11.32	5.08
MLLE [50]	18.82	1.12	15.05	2.45	15.06	2.32
UNTV [51]	16.57	1.88	17.12	1.42	17.50	1.39
SPDF [52]	**19.85**	**0.92**	17.57	1.37	18.82	1.09
deep-sesr [41]	15.77	2.08	**23.22**	**0.38**	**23.22**	**0.35**
FUnIE-GAN [5]	18.07	1.78	**22.97**	**0.41**	**23.53**	**0.41**
WaterNet [2]	19.81	1.02	19.63	0.83	20.58	0.71
UWCNN [28]	13.26	4.00	16.41	1.98	17.72	1.40
JI-Net [38]	18.21	2.46	16.54	1.78	–	–
ACPAB [35]	15.20	2.52	17.04	1.73	18.06	1.40
TOPAL [37]	**19.85**	0.93	19.31	0.83	19.98	0.75
Ucolor [6]	**20.61**	**0.78**	19.45	0.85	20.08	0.76
PUGAN	**21.67**	**0.54**	**23.70**	**0.32**	**24.05**	**0.34**

Experiments

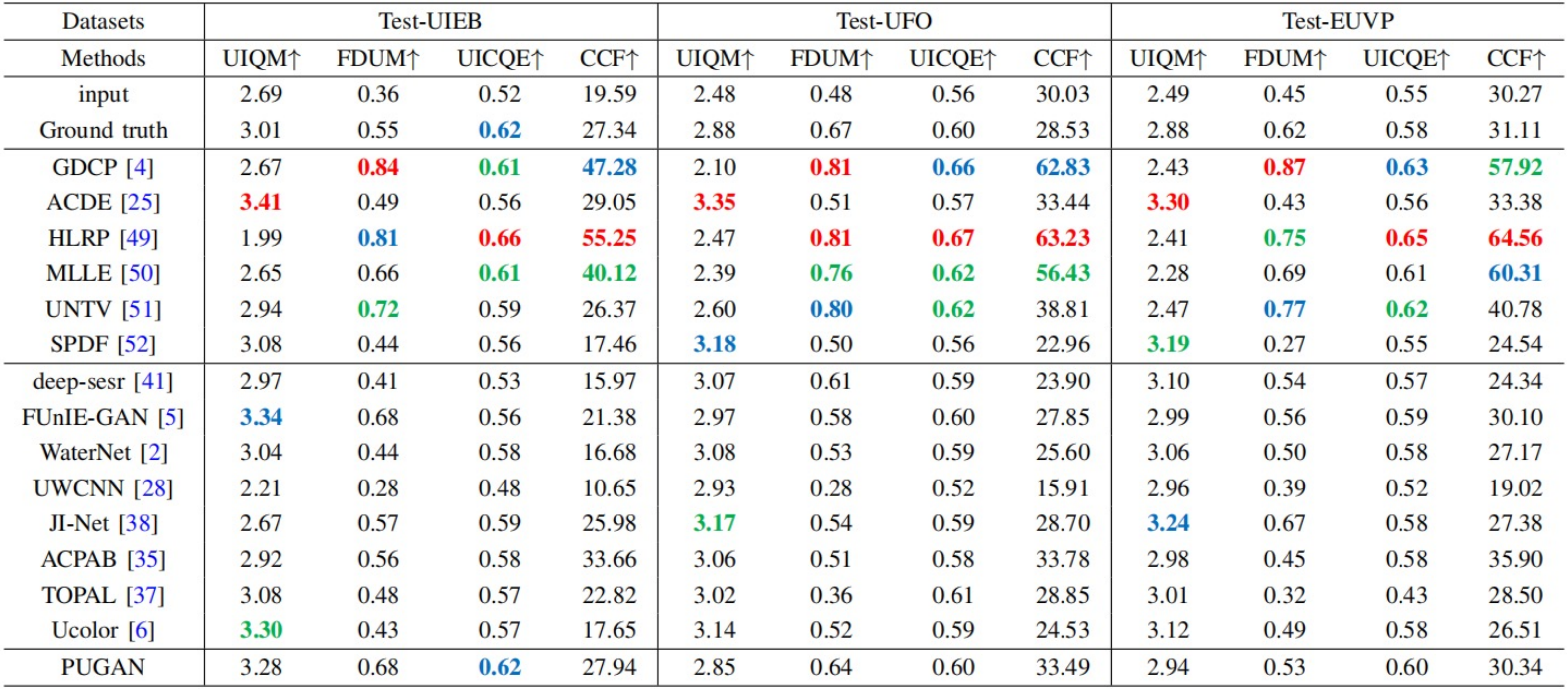

Datasets	Test-UIEB				Test-UFO				Test-EUVP			
Methods	UIQM↑	FDUM↑	UICQE↑	CCF↑	UIQM↑	FDUM↑	UICQE↑	CCF↑	UIQM↑	FDUM↑	UICQE↑	CCF↑
input	2.69	0.36	0.52	19.59	2.48	0.48	0.56	30.03	2.49	0.45	0.55	30.27
Ground truth	3.01	0.55	**0.62**	27.34	2.88	0.67	0.60	28.53	2.88	0.62	0.58	31.11
GDCP [4]	2.67	**0.84**	**0.61**	**47.28**	2.10	**0.81**	**0.66**	**62.83**	2.43	**0.87**	**0.63**	**57.92**
ACDE [25]	**3.41**	0.49	0.56	29.05	**3.35**	0.51	0.57	33.44	**3.30**	0.43	0.56	33.38
HLRP [49]	1.99	**0.81**	**0.66**	**55.25**	2.47	**0.81**	**0.67**	**63.23**	2.41	**0.75**	**0.65**	**64.56**
MLLE [50]	2.65	0.66	**0.61**	**40.12**	2.39	**0.76**	**0.62**	**56.43**	2.28	0.69	0.61	**60.31**
UNTV [51]	2.94	**0.72**	0.59	26.37	2.60	**0.80**	**0.62**	38.81	2.47	**0.77**	**0.62**	40.78
SPDF [52]	3.08	0.44	0.56	17.46	**3.18**	0.50	0.56	22.96	**3.19**	0.27	0.55	24.54
deep-sesr [41]	2.97	0.41	0.53	15.97	3.07	0.61	0.59	23.90	3.10	0.54	0.57	24.34
FUnIE-GAN [5]	**3.34**	0.68	0.56	21.38	2.97	0.58	0.60	27.85	2.99	0.56	0.59	30.10
WaterNet [2]	3.04	0.44	0.58	16.68	3.08	0.53	0.59	25.60	3.06	0.50	0.58	27.17
UWCNN [28]	2.21	0.28	0.48	10.65	2.93	0.28	0.52	15.91	2.96	0.39	0.52	19.02
JI-Net [38]	2.67	0.57	0.59	25.98	**3.17**	0.54	0.59	28.70	**3.24**	0.67	0.58	27.38
ACPAB [35]	2.92	0.56	0.58	33.66	3.06	0.51	0.58	33.78	2.98	0.45	0.58	35.90
TOPAL [37]	3.08	0.48	0.57	22.82	3.02	0.36	0.61	28.85	3.01	0.32	0.43	28.50
Ucolor [6]	**3.30**	0.43	0.57	17.65	3.14	0.52	0.59	24.53	3.12	0.49	0.58	26.51
PUGAN	3.28	0.68	**0.62**	27.94	2.85	0.64	0.60	33.49	2.94	0.53	0.60	30.34

Experiments

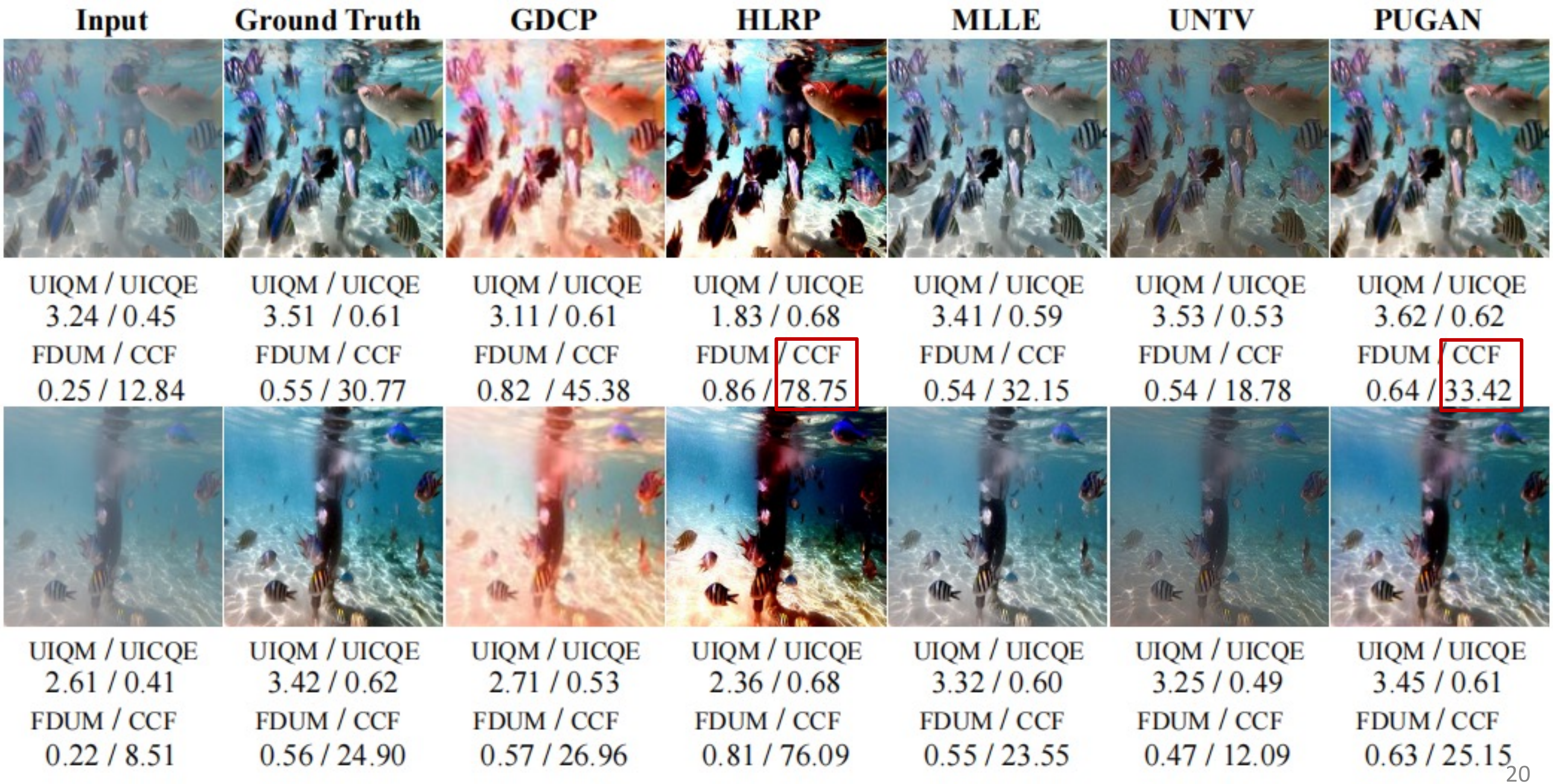

	Input	Ground Truth	GDCP	HLRP	MLLE	UNTV	PUGAN
	UIQM / UICQE	UIQM / UICQE	UIQM / UICQE	UIQM / UICQE	UIQM / UICQE	UIQM / UICQE	UIQM / UICQE
	3.24 / 0.45	3.51 / 0.61	3.11 / 0.61	1.83 / 0.68	3.41 / 0.59	3.53 / 0.53	3.62 / 0.62
	FDUM / CCF	FDUM / CCF	FDUM / CCF	FDUM / CCF	FDUM / CCF	FDUM / CCF	FDUM / CCF
	0.25 / 12.84	0.55 / 30.77	0.82 / 45.38	0.86 / 78.75	0.54 / 32.15	0.54 / 18.78	0.64 / 33.42
	UIQM / UICQE	UIQM / UICQE	UIQM / UICQE	UIQM / UICQE	UIQM / UICQE	UIQM / UICQE	UIQM / UICQE
	2.61 / 0.41	3.42 / 0.62	2.71 / 0.53	2.36 / 0.68	3.32 / 0.60	3.25 / 0.49	3.45 / 0.61
	FDUM / CCF	FDUM / CCF	FDUM / CCF	FDUM / CCF	FDUM / CCF	FDUM / CCF	FDUM / CCF
	0.22 / 8.51	0.56 / 24.90	0.57 / 26.96	0.81 / 76.09	0.55 / 23.55	0.47 / 12.09	0.63 / 25.15

Ablation Study

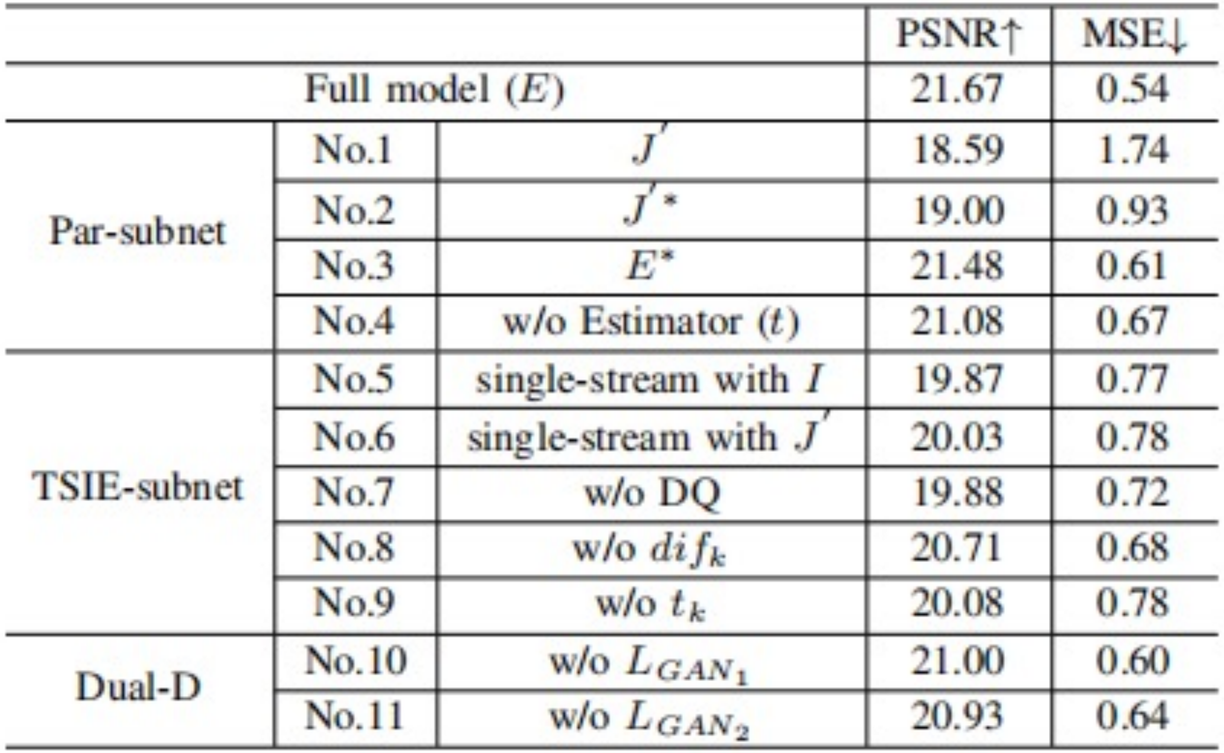

			PSNR↑	MSE↓
Full model (E)			21.67	0.54
Par-subnet	No.1	J'	18.59	1.74
	No.2	J'^*	19.00	0.93
	No.3	E^*	21.48	0.61
	No.4	w/o Estimator (t)	21.08	0.67
TSIE-subnet	No.5	single-stream with I	19.87	0.77
	No.6	single-stream with J'	20.03	0.78
	No.7	w/o DQ	19.88	0.72
	No.8	w/o dif_k	20.71	0.68
	No.9	w/o t_k	20.08	0.78
Dual-D	No.10	w/o L_{GAN_1}	21.00	0.60
	No.11	w/o L_{GAN_2}	20.93	0.64

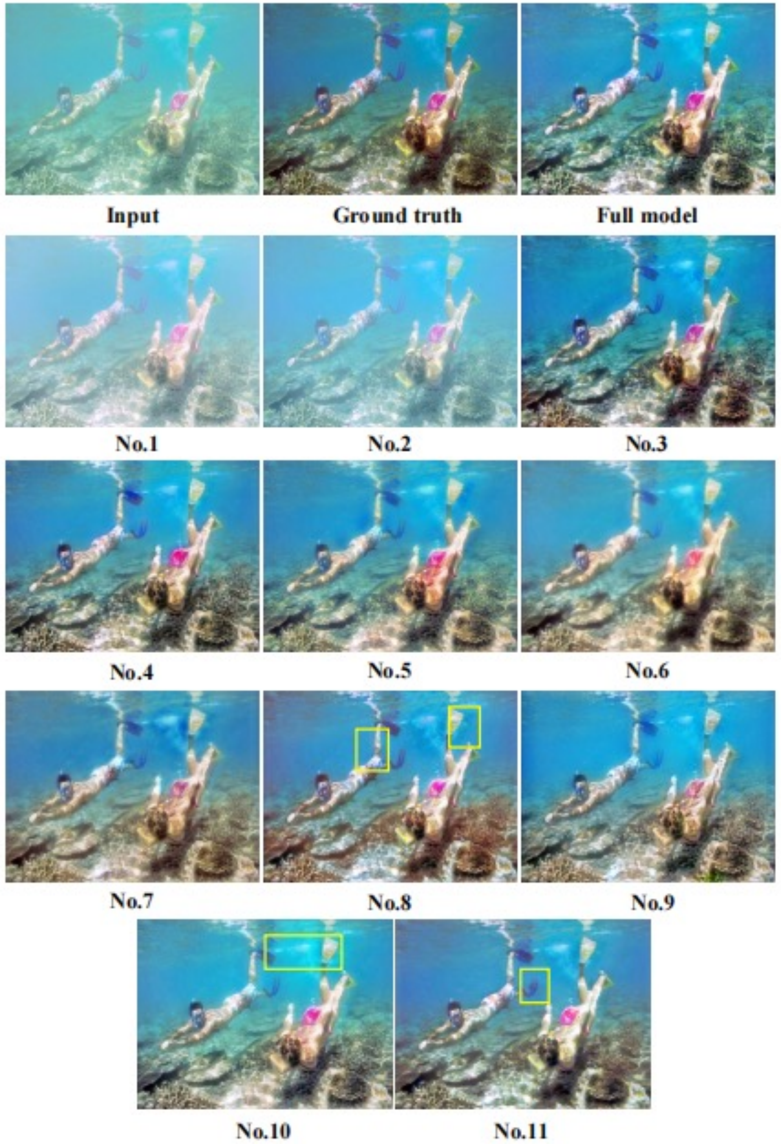

Conclusion

- In this paper, we propose a **physical model-guided GAN model** for underwater image enhancement.
- In the phy-G, we fully combine the physical model and the CNN-based model, where the **Par-subnet** generates the color enhanced underwater image by physical inversion, and the **TSIE-subnet** equipped with a DQ module aims to generate the final enhanced image through the regional and differential feature learning.
- In addition, we design a novel **Dual-D structure** to judge the reconstruction results of the generator, following a style-content synergy mechanism.
- Our extensive experiments on different benchmarks demonstrate the superiority of this method and the effectiveness of each module.

水下环境内容理解

Underwater Environment Content Understanding

ICCV23
PARIS

WaterMask: Instance Segmentation for Underwater Imagery

Shijie Lian, Hua Li, Runmin Cong, Suqi Li, Wei Zhang, and Sam Kwong*

*IEEE International Conference on Computer Vision, **2023***

https://github.com/LiamLian0727/WaterMask

Introduction

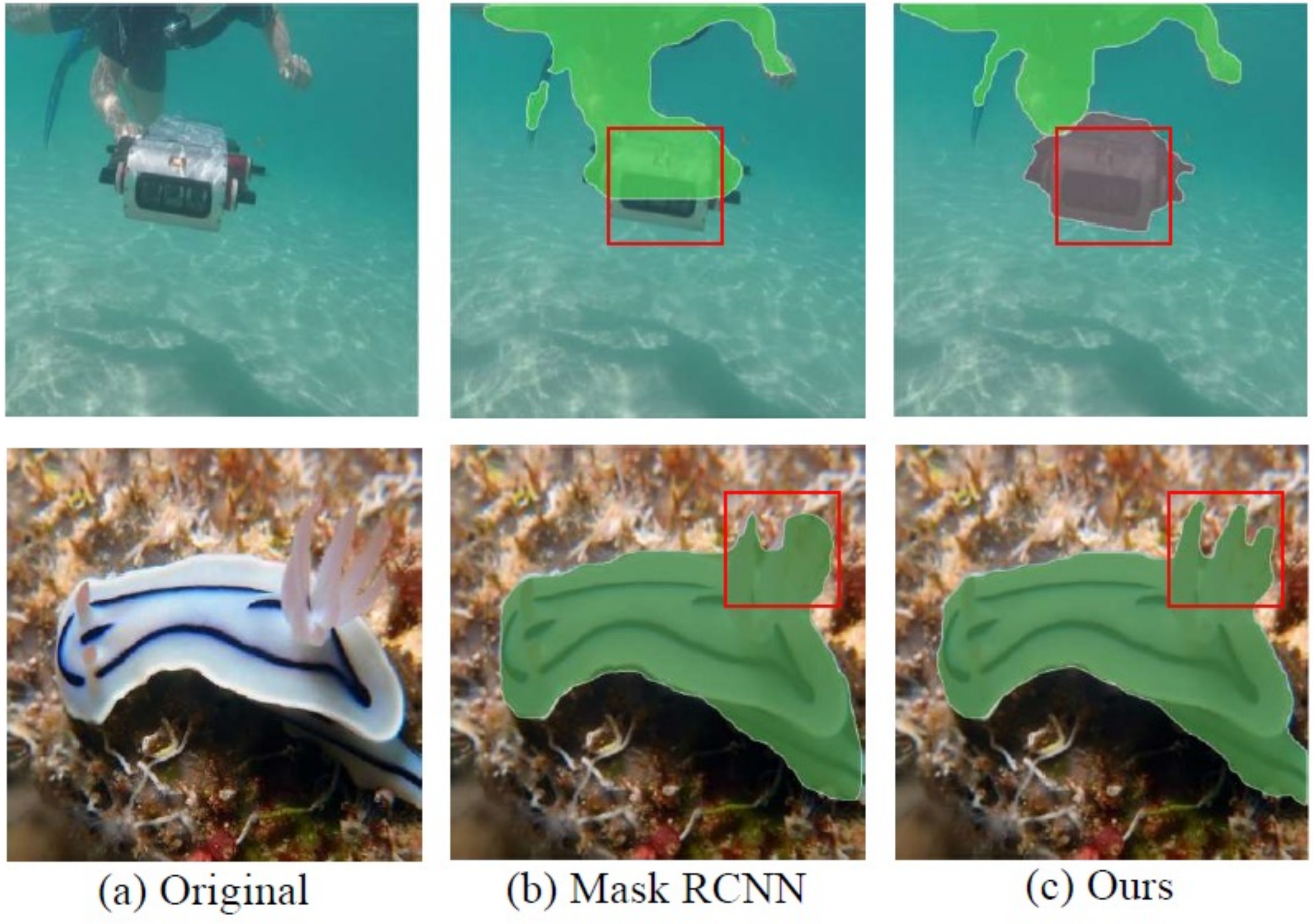

- Since instance segmentation is valuable in estimating object interactions and inferring scene geometry, it is of great use in many underwater vision scenarios such as underwater robot vision and underwater vehicle autopilot.
- However, the segmentation of image instances for general underwater scenes has not been thoroughly explored. The results of directly applying natural image segmentation models to underwater images with generally degraded quality are often unsatisfactory!

Motivation

- On the one hand, there is **no general underwater image instance segmentation dataset** to promote training and evaluation of instance segmentation models. On the other hand, quality degradation of underwater images is inevitable due to wavelength and distance-related attenuation and scattering. **Low-quality images** often lead to the **failure of current segmentation methods**.
- To alleviate this issue, we propose the **first underwater image instance segmentation (UIIS) dataset**, aiming to promote the development of instance segmentation for underwater tasks.
- Simultaneously, we propose **WaterMask** for multi-object underwater image instance segmentation according to the **intrinsic characteristics of underwater imagery**.

Contributions

a) We construct the first general underwater image instance segmentation (UIIS) dataset **containing 4,628 images for 7 categories with pixel-level annotations** for underwater instance segmentation task.

b) We propose the **first underwater instance segmentation model WaterMask**, as far as we know. In WaterMask, we devise **DSGAT and MFRM modules** to **reconstruct and refine** the image features with underwater imaging degradation, and Boundary Mask Strategy with boundary learning loss to **optimize the boundaries** of underwater clustered instances.

c) Extensive experiments on popular evaluation criteria demonstrate the **effectiveness** of the proposed UIIS dataset and WaterMask.

Our UIIS Dataset

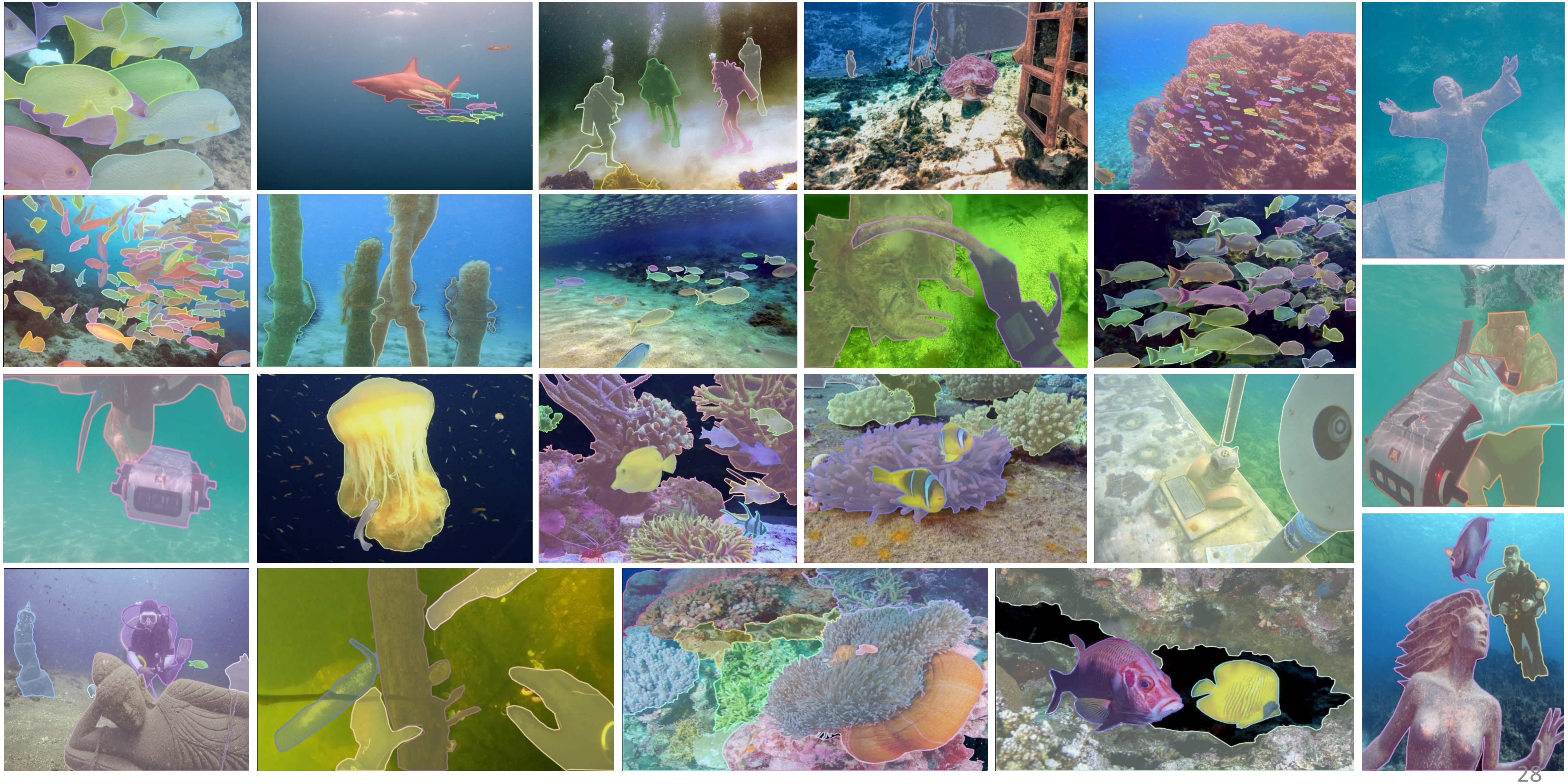

Dataset Statistic and Challenges

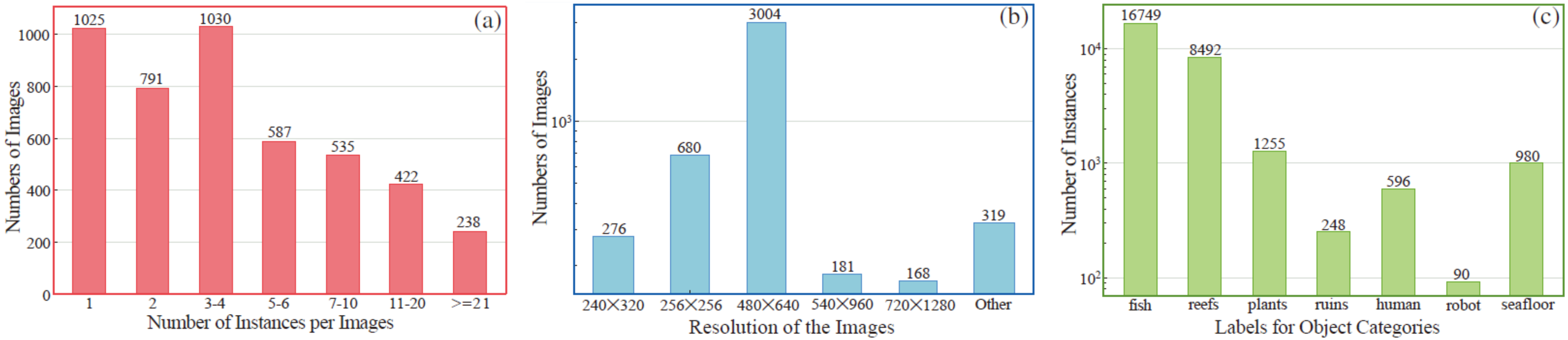

➢ **Challenge in the number of instance.**

We counted the number of instances in the dataset and the scenes with more than 5 instances accounted for 38.5% of the total and more than 10 instances accounted for 14.2%, in which the image with the most instances had 162 instances.

➢ **Challenges in small or large instances.**

UIIS dataset have 3319 instances less than 14×14 pixels, accounting for 11.7% of the total, in addition to 6485 instances of size larger than 128x128 pixels, accounting for 22.8% of the total.

➢ **Challenges in various image resolutions and image scenarios.**

Contains images of various resolutions to match handheld camera shots or industrial equipment shots.

Contains images with significantly degraded quality, high saturation or high contrast images to evaluate the performance of the network in different ocean scenarios.

WaterMask

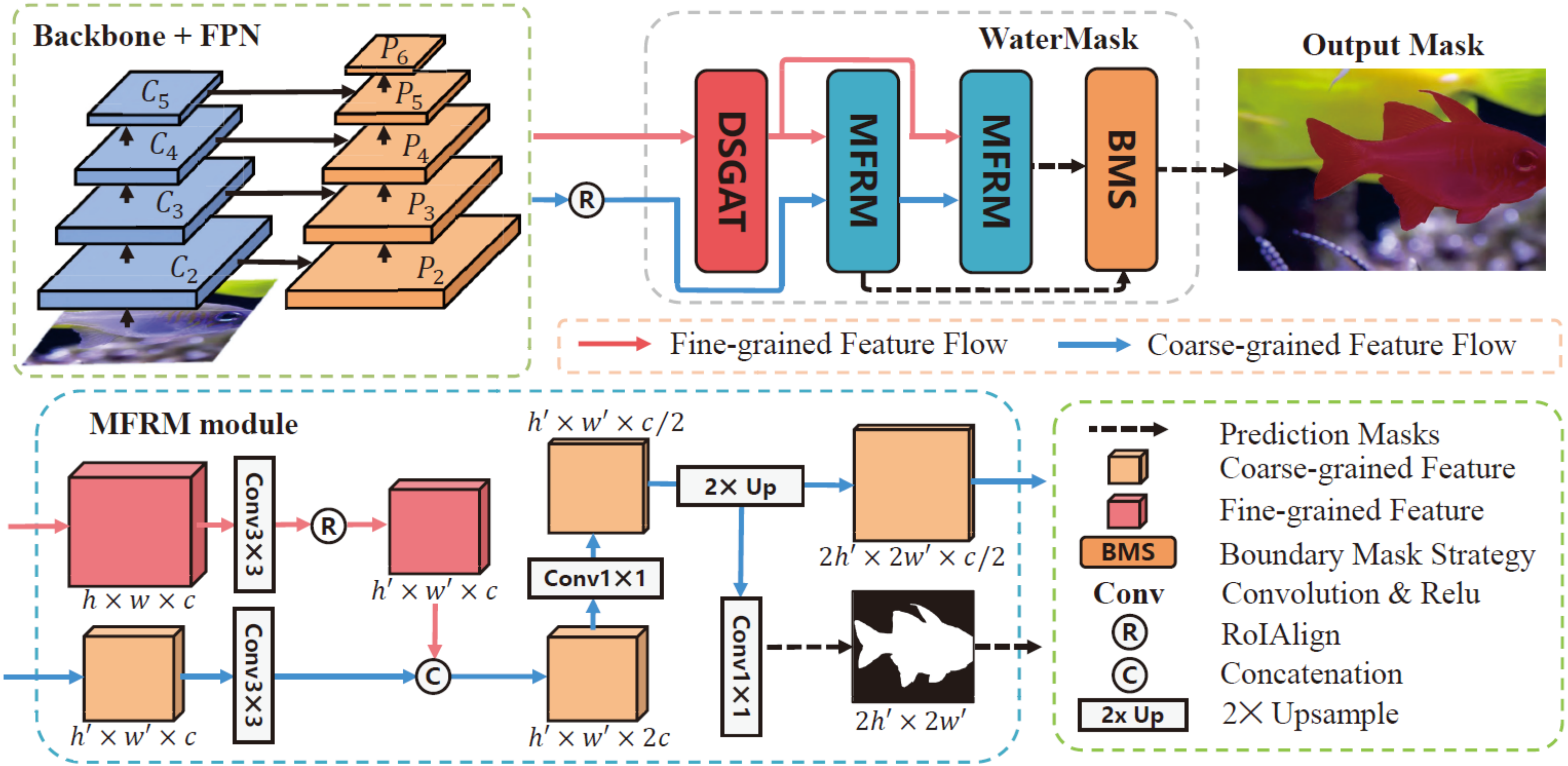

Backbone + FPN
C_5
C_4
C_3
C_2
P_6
P_5
P_4
P_3
P_2
R
WaterMask
DSGAT
MFRM
MFRM
BMS
Output Mask
Fine-grained Feature Flow
Coarse-grained Feature Flow
MFRM module
$h \times w \times c$
Conv3×3
R
$h' \times w' \times c$
$h' \times w' \times c/2$
2× Up
$2h' \times 2w' \times c/2$
Conv1×1
$h' \times w' \times c$
Conv3×3
C
$h' \times w' \times 2c$
Conv1×1
$2h' \times 2w'$
Prediction Masks
Coarse-grained Feature
Fine-grained Feature
BMS
Boundary Mask Strategy
Conv
Convolution & Relu
R
RoIAlign
C
Concatenation
2x Up
2× Upsample

Difference Similarity Graph Attention Module

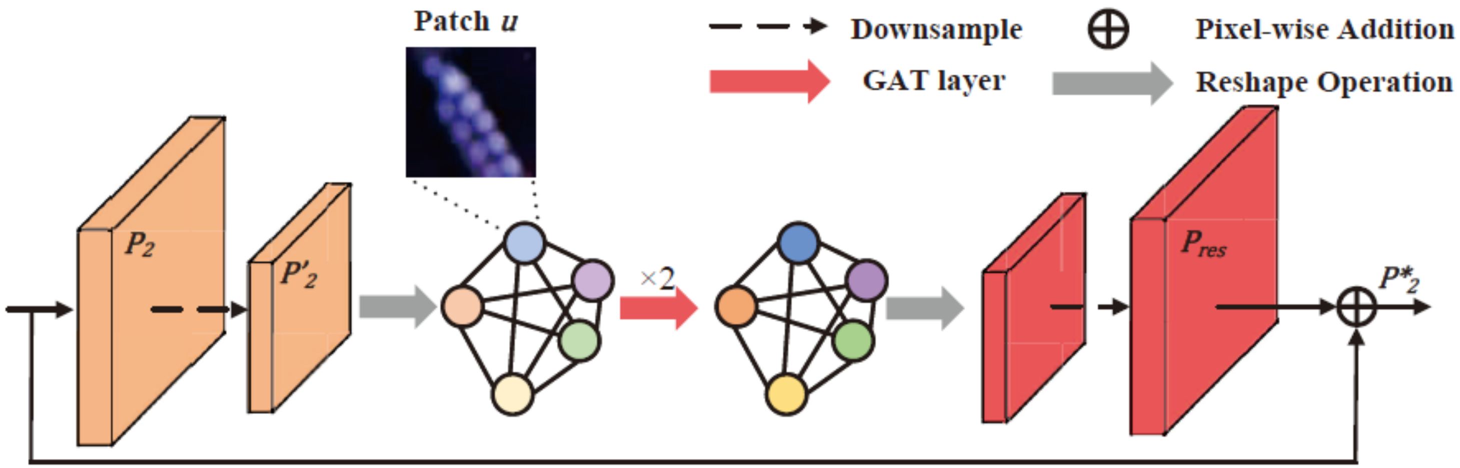

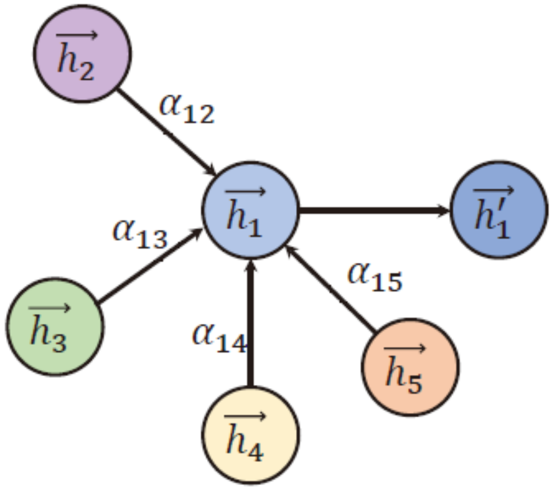

Although underwater images generally suffer from quality degradation, underwater instances are mostly clustered, which makes it possible for underwater images to have similar visual information in multiple places, retaining different degraded details under different water and lighting conditions. Therefore, we propose DSGAT for collecting this similar visual information by computing the attention between image patches so that each patch can be complemented by the visual information of multiple other similar patches, and reconstructing the image details by extracting and combining information through GAT operations.

$$a_{ij} = \frac{exp(\sigma(l^{\mathrm{T}}[W\vec{h_i} \parallel W\vec{h_j}]))}{\sum_{n \in \mathcal{N}_i} exp(\sigma(l^{\mathrm{T}}[W\vec{h_i} \parallel W\vec{h_n}]))},$$

$$\vec{h'_i} = \delta(\sum_{n \in \mathcal{N}_i} a_{ij} W \vec{h_j}).$$

Multi-level Feature Refinement Module

We then design the **Multi-level Feature Refinement Module (MFRM)**, which infers different resolution masks by supplementing the degradation information so that **higher resolution features can be utilized** to fully predict the boundaries.

MFRM sends the features extracted from the feature pyramid by 14×14 RoIAlign operation to two 3×3 convolutional layers to generate the **initial instance feature F1**. After that, we utilize the fine-grained features generated by DSGAT to iteratively refine the initial F1 by MFRM.

The MFRM will be executed twice, outputting features F2 and F3, which will be used as foreground and boundary predictions, respectively.

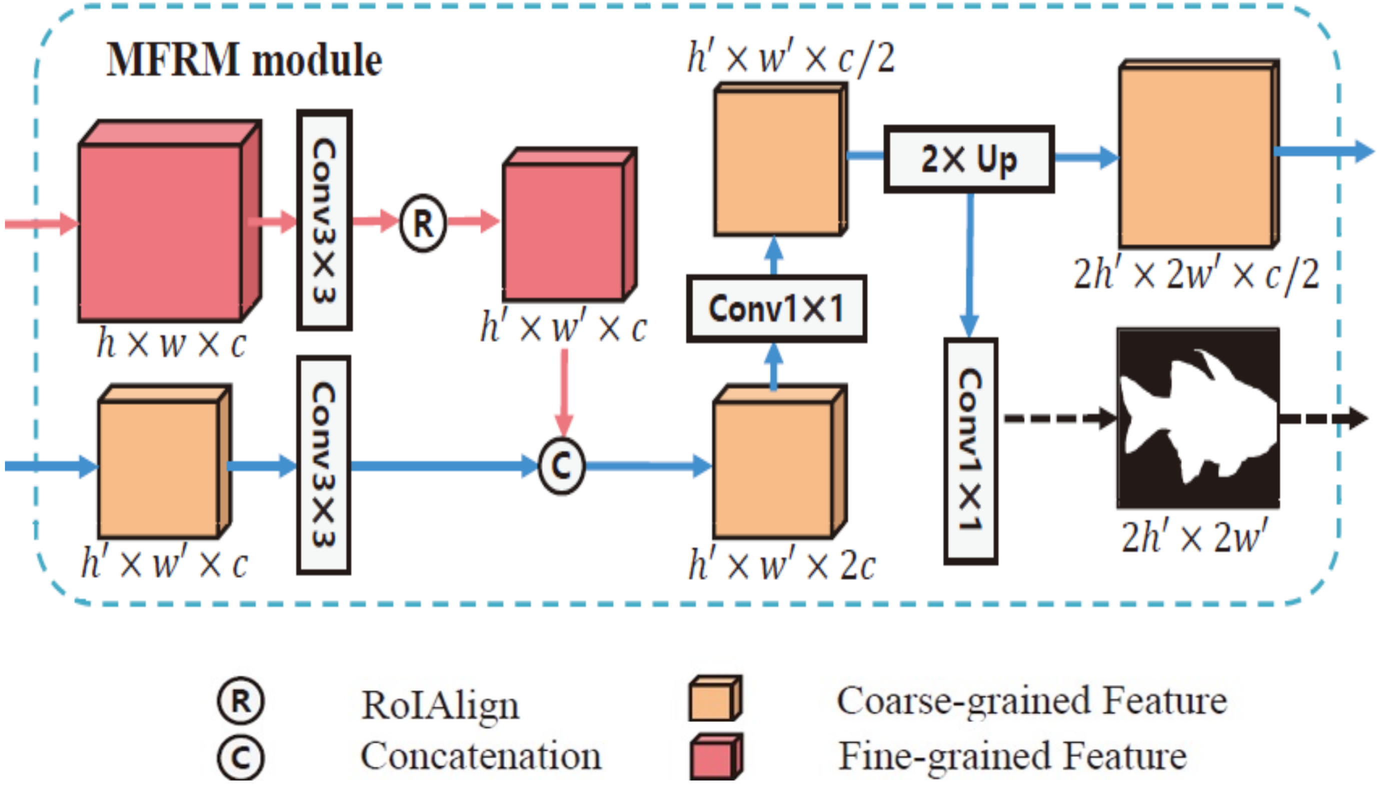

Boundary Mask Strategy

We feed the features F2 and F3 into the 1×1 convolution layer to generate instance masks M2 and M3 with different resolutions. The pixels in F2 have a large receptive field and contain rich high-level information, which is beneficial for predicting the approximate location of the instance mask, but because of the low feature resolution, the boundaries of the prediction results tend to be rough. Conversely, F3, while the high-resolution mask reduces the boundary error, also causes the network to overpredict other pixels of the mask. Therefore, we use M2 and M3 to splice our output together, with $B_{2\times} = f_{2\times}(B(M_2))$ and $R_{2\times} = f_{2\times}(B(M_2) \vee B(G_2))$ in the following equation.

Boundary Learning Loss

The boundaries of underwater instances are often blurred, and the pixels used for training boundary classification are much smaller than those used for mask classification, leading to the fact that the commonly used BCE loss is not effective in helping the network to learn information from the boundary. We design the Boundary Learning Loss (BLL) to assign more weights to the boundary regions, thus forcing the network to pay more attention to the classification within the boundary pixels and thus make more accurate predictions.

Calculated Output:

$$p_{ij} = \begin{cases} b^2 - 1, & \text{if } i = j = \frac{b-1}{2} \\ -1, & \text{otherwise,} \end{cases} \qquad B(M) = \begin{cases} 1, & \text{if } \left|\nabla^2 p(M)\right| \leq \mu b^2 \\ 0, & \text{otherwise,} \end{cases}$$

$$M_{out} = f_{2\times}(M_2) \odot B_{2\times} + M_3 \odot (1 - B_{2\times})$$

Loss Function:

$$\mathcal{L}_B = \frac{\sum_i^{H\times W} R_{2\times}^i \cdot BCE\left(M_3^i, G_3^i\right)}{\sum_i^{H\times W} R_{2\times}^i} \qquad \mathcal{L}_{mask} = \mathcal{L}_B + \sum_{k \subset [1,2]} \lambda_k \mathcal{L}_{BCE}(M_k, G_k)$$

Experiments

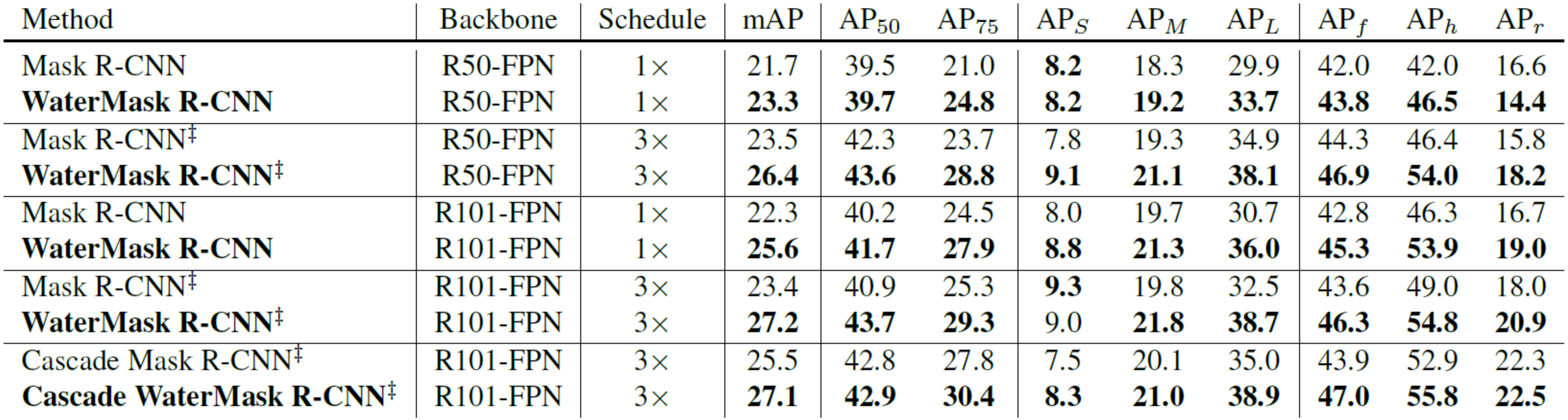

Method	Backbone	Schedule	mAP	AP$_{50}$	AP$_{75}$	AP$_S$	AP$_M$	AP$_L$	AP$_f$	AP$_h$	AP$_r$
Mask R-CNN	R50-FPN	1×	21.7	39.5	21.0	**8.2**	18.3	29.9	42.0	42.0	16.6
WaterMask R-CNN	R50-FPN	1×	**23.3**	**39.7**	**24.8**	**8.2**	**19.2**	**33.7**	**43.8**	**46.5**	**14.4**
Mask R-CNN‡	R50-FPN	3×	23.5	42.3	23.7	7.8	19.3	34.9	44.3	46.4	15.8
WaterMask R-CNN‡	R50-FPN	3×	**26.4**	**43.6**	**28.8**	**9.1**	**21.1**	**38.1**	**46.9**	**54.0**	**18.2**
Mask R-CNN	R101-FPN	1×	22.3	40.2	24.5	8.0	19.7	30.7	42.8	46.3	16.7
WaterMask R-CNN	R101-FPN	1×	**25.6**	**41.7**	**27.9**	**8.8**	**21.3**	**36.0**	**45.3**	**53.9**	**19.0**
Mask R-CNN‡	R101-FPN	3×	23.4	40.9	25.3	**9.3**	19.8	32.5	43.6	49.0	18.0
WaterMask R-CNN‡	R101-FPN	3×	**27.2**	**43.7**	**29.3**	9.0	**21.8**	**38.7**	**46.3**	**54.8**	**20.9**
Cascade Mask R-CNN‡	R101-FPN	3×	25.5	42.8	27.8	7.5	20.1	35.0	43.9	52.9	22.3
Cascade WaterMask R-CNN‡	R101-FPN	3×	**27.1**	**42.9**	**30.4**	**8.3**	**21.0**	**38.9**	**47.0**	**55.8**	**22.5**

Table 2: Comparison with Mask R-CNN and Cascade Mask R-CNN on UIIS dataset. Models with ‡ were trained with 3× schedule using multi-scale training.

Experiments

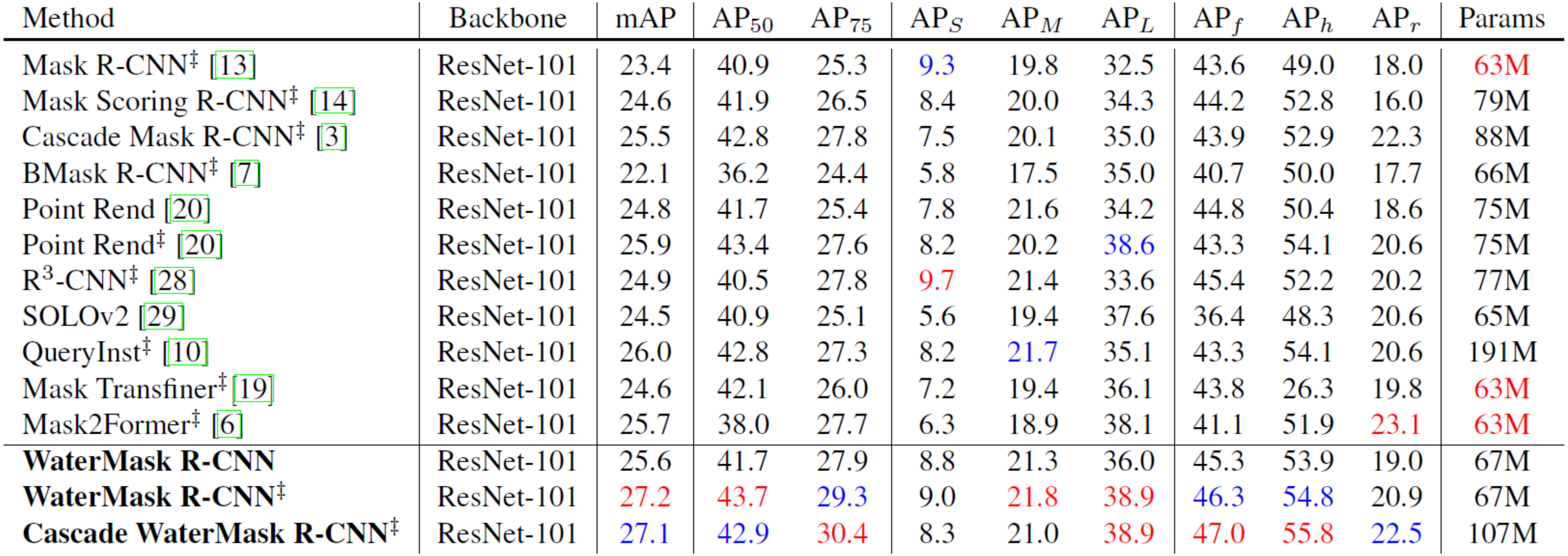

Method	Backbone	mAP	AP_{50}	AP_{75}	AP_S	AP_M	AP_L	AP_f	AP_h	AP_r	Params
Mask R-CNN‡ [13]	ResNet-101	23.4	40.9	25.3	9.3	19.8	32.5	43.6	49.0	18.0	63M
Mask Scoring R-CNN‡ [14]	ResNet-101	24.6	41.9	26.5	8.4	20.0	34.3	44.2	52.8	16.0	79M
Cascade Mask R-CNN‡ [3]	ResNet-101	25.5	42.8	27.8	7.5	20.1	35.0	43.9	52.9	22.3	88M
BMask R-CNN‡ [7]	ResNet-101	22.1	36.2	24.4	5.8	17.5	35.0	40.7	50.0	17.7	66M
Point Rend [20]	ResNet-101	24.8	41.7	25.4	7.8	21.6	34.2	44.8	50.4	18.6	75M
Point Rend‡ [20]	ResNet-101	25.9	43.4	27.6	8.2	20.2	38.6	43.3	54.1	20.6	75M
R^3-CNN‡ [28]	ResNet-101	24.9	40.5	27.8	9.7	21.4	33.6	45.4	52.2	20.2	77M
SOLOv2 [29]	ResNet-101	24.5	40.9	25.1	5.6	19.4	37.6	36.4	48.3	20.6	65M
QueryInst‡ [10]	ResNet-101	26.0	42.8	27.3	8.2	21.7	35.1	43.3	54.1	20.6	191M
Mask Transfiner‡ [19]	ResNet-101	24.6	42.1	26.0	7.2	19.4	36.1	43.8	26.3	19.8	63M
Mask2Former‡ [6]	ResNet-101	25.7	38.0	27.7	6.3	18.9	38.1	41.1	51.9	23.1	63M
WaterMask R-CNN	ResNet-101	25.6	41.7	27.9	8.8	21.3	36.0	45.3	53.9	19.0	67M
WaterMask R-CNN‡	ResNet-101	27.2	43.7	29.3	9.0	21.8	38.9	46.3	54.8	20.9	67M
Cascade WaterMask R-CNN‡	ResNet-101	27.1	42.9	30.4	8.3	21.0	38.9	47.0	55.8	22.5	107M

Table 3: Comparison with the State-of-the-art Methods on UIIS. Models with ‡ were trained with 3× schedule using multi-scale training. The data marked in red are the best, and those in blue are the second best.

Experiments

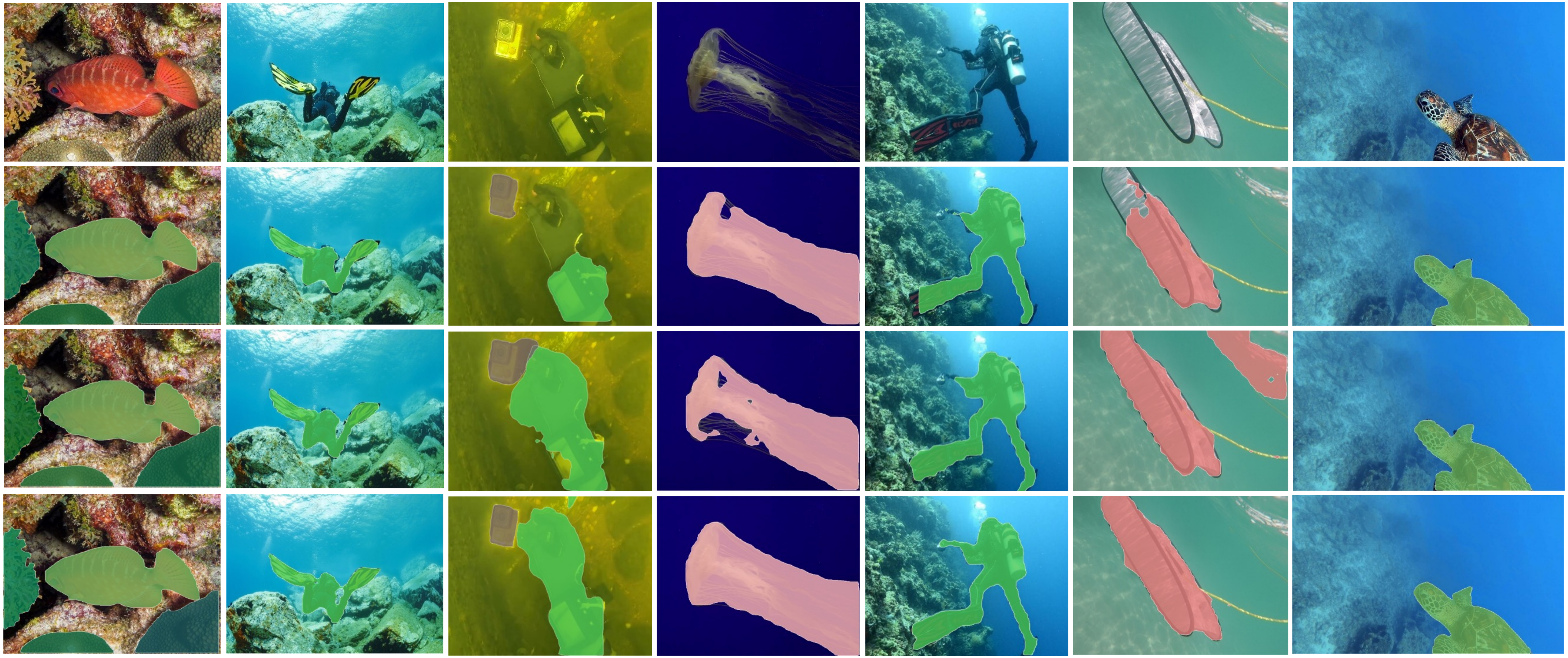

Figure 1: Qualitative comparison on the UIIS dataset. The first row represents the original image, and the second, third and fourth rows represent the results of Mask R-CNN, QueryInst and ours, respectively.

Ablation Study

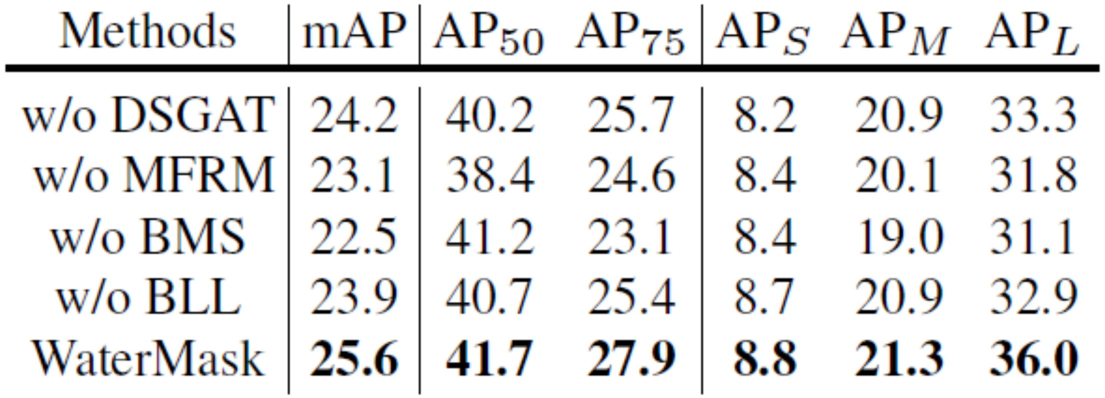

Methods	mAP	AP$_{50}$	AP$_{75}$	AP$_S$	AP$_M$	AP$_L$
w/o DSGAT	24.2	40.2	25.7	8.2	20.9	33.3
w/o MFRM	23.1	38.4	24.6	8.4	20.1	31.8
w/o BMS	22.5	41.2	23.1	8.4	19.0	31.1
w/o BLL	23.9	40.7	25.4	8.7	20.9	32.9
WaterMask	**25.6**	**41.7**	**27.9**	**8.8**	**21.3**	**36.0**

Table 4: Effectiveness of each component in WaterMask. ResNet-101-FPN and 1× training schedule is adopted.

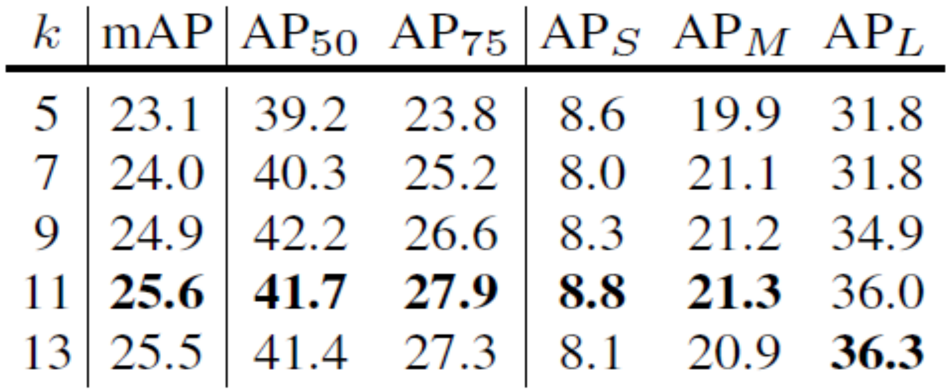

k	mAP	AP$_{50}$	AP$_{75}$	AP$_S$	AP$_M$	AP$_L$
5	23.1	39.2	23.8	8.6	19.9	31.8
7	24.0	40.3	25.2	8.0	21.1	31.8
9	24.9	42.2	26.6	8.3	21.2	34.9
11	**25.6**	**41.7**	**27.9**	**8.8**	**21.3**	36.0
13	25.5	41.4	27.3	8.1	20.9	**36.3**

Table 5: Different value of k. k is the number of farthest nodes to be connected.

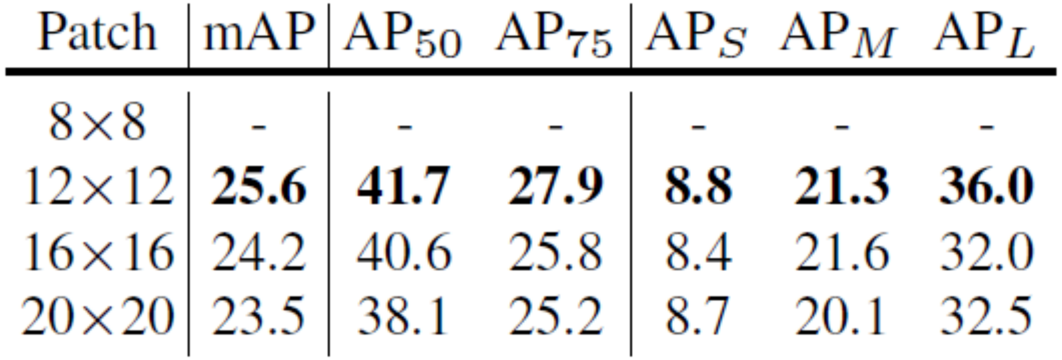

Patch	mAP	AP$_{50}$	AP$_{75}$	AP$_S$	AP$_M$	AP$_L$
8×8	-	-	-	-	-	-
12×12	**25.6**	**41.7**	**27.9**	**8.8**	**21.3**	**36.0**
16×16	24.2	40.6	25.8	8.4	21.6	32.0
20×20	23.5	38.1	25.2	8.7	20.1	32.5

Table 6: Different Size of Patch. Each graph node corresponds to a 4s × 4s patch, where s is downsampling stride. When s = 2, the memory required by the model has exceeded the upper limit of the device.

Conclusion and Future Work

- In this paper, we have constructed the first general underwater image instance segmentation dataset with pixel-level annotations, which enables us to comprehensively explore the underwater instance segmentation task.

- According to the intrinsic characteristics of underwater imagery, we have proposed WaterMask for underwater instance segmentation. Extensive experiments have demonstrated the effectiveness of the proposed UIIS dataset and WaterMask.

- In future work, we plan to extend the UIIS datasets to broader and more challenging underwater images and underwater videos.

Diving into Underwater: Segment Anything Model Guided Underwater Salient Instance Segmentation and A Large-scale Dataset

Shijie Lian, Ziyi Zhang, Hua Li, Wenjie Li, Tianruo Yang, Sam Kwong, Runmin Cong

IEEE International Conference on Machine Learning, 2024

https://github.com/LiamLian0727/USIS10K

Introduction

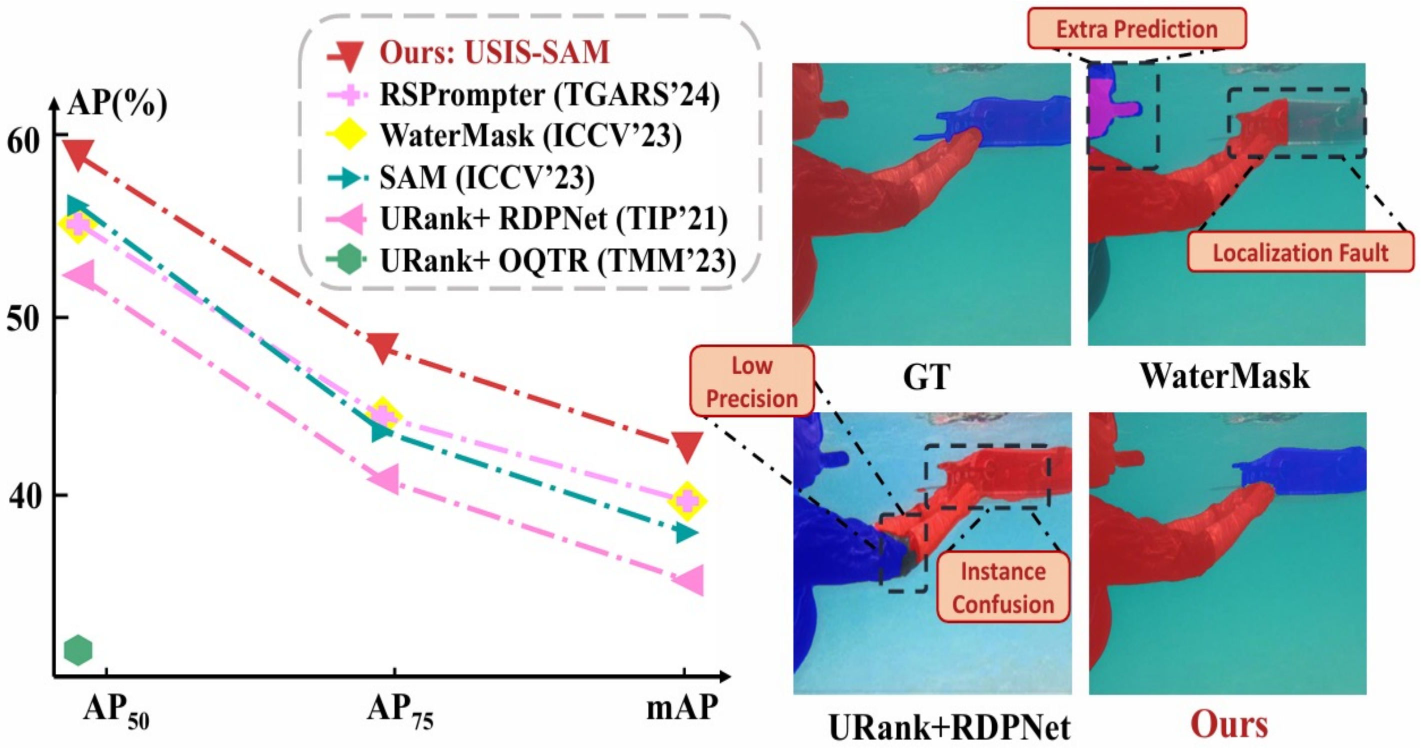

- ➢ **Salient Instance Segmentation (SIS)**, an emerging and promising visual task, aims to segment out visually salient objects in a scene and distinguish individual salient instances, which is beneficial for vision tasks such as marine resource exploration and underwater human-computer interaction.

- ➢ However, directly transferring conventional SIS methods for land images to underwater scenes may struggle to achieve ideal performance attribute to the **domain gap** of **intrinsic characteristics and extrinsic circumstances between land and underwater living**.

Motivation

- On the one hand, there is **no general underwater salient image instance segmentation dataset** to promote training and evaluation of the underwater salient instance segmentation models.
- On the other hand, even state-of-the-art SIS models trained on large-scale land-based datasets coupled with the best underwater image enhancement algorithms **cannot achieve satisfactory performance in underwater environments**.
- To alleviate this issue, we construct the **first large-scale underwater salient instance segmentation (USIS) dataset**, **USIS10K**, aiming to promote the development of salient instance segmentation for underwater tasks.
- Simultaneously, we first attempt to apply Segment Anything Model (SAM) to underwater salient instance segmentation and propose **USIS-SAM**, aiming to **improve the segmentation accuracy in complex underwater scenes**.

Contributions

a) We construct the **first large-scale dataset, USIS10K**, for the underwater salient instance segmentation task, which contains **10,632 images and pixel-level annotations of 7 categories**. As far as we know, this is **the largest salient instance segmentation dataset**, and includes Class-Agnostic and Multi-Class labels simultaneously.

b) We propose the **first underwater salient instance segmentation model, USIS-SAM**, as far as we know. In USIS-SAM, we design **Underwater Adaptive ViT Encoder** to incorporate underwater visual prompts into network via adapters, and **Salient Feature Prompter Generator** to automatically generate salient prompters, guiding an end-to-end segmentation network.

c) Extensive public evaluation criteria and large numbers of experiments verify the effectiveness of our USIS10K dataset and USIS-SAM.

USIS10K Dataset

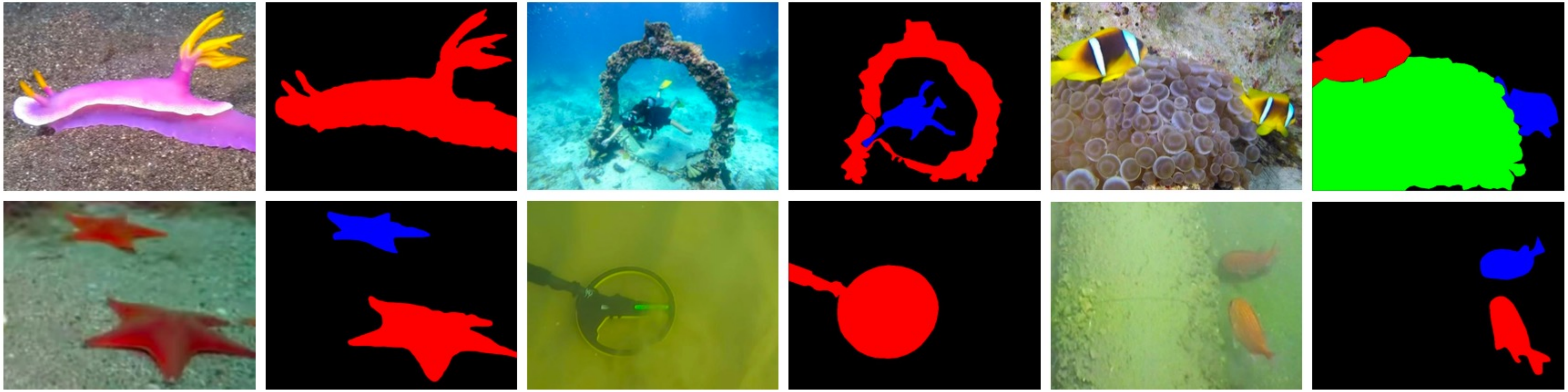

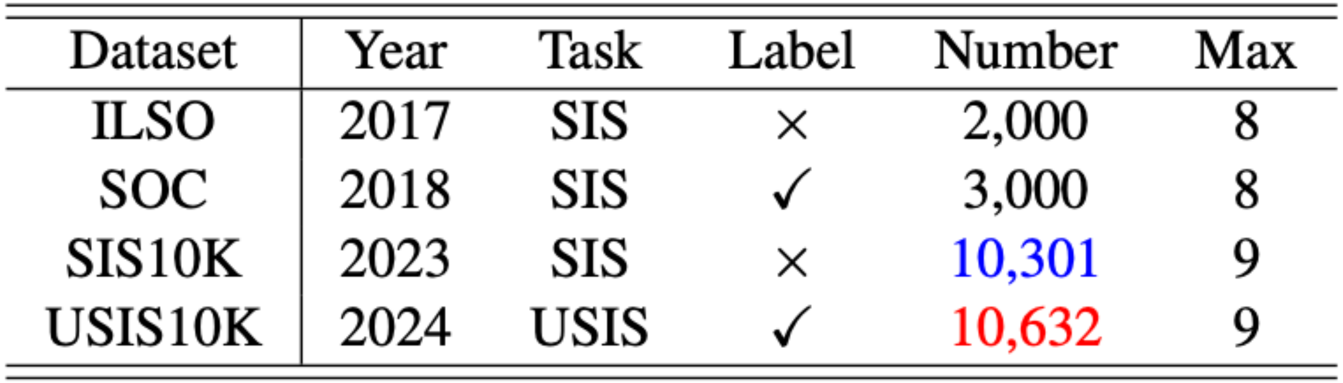

Dataset	Year	Task	Label	Number	Max
ILSO	2017	SIS	×	2,000	8
SOC	2018	SIS	✓	3,000	8
SIS10K	2023	SIS	×	10,301	9
USIS10K	2024	USIS	✓	10,632	9

Dataset Statistic and Challenges

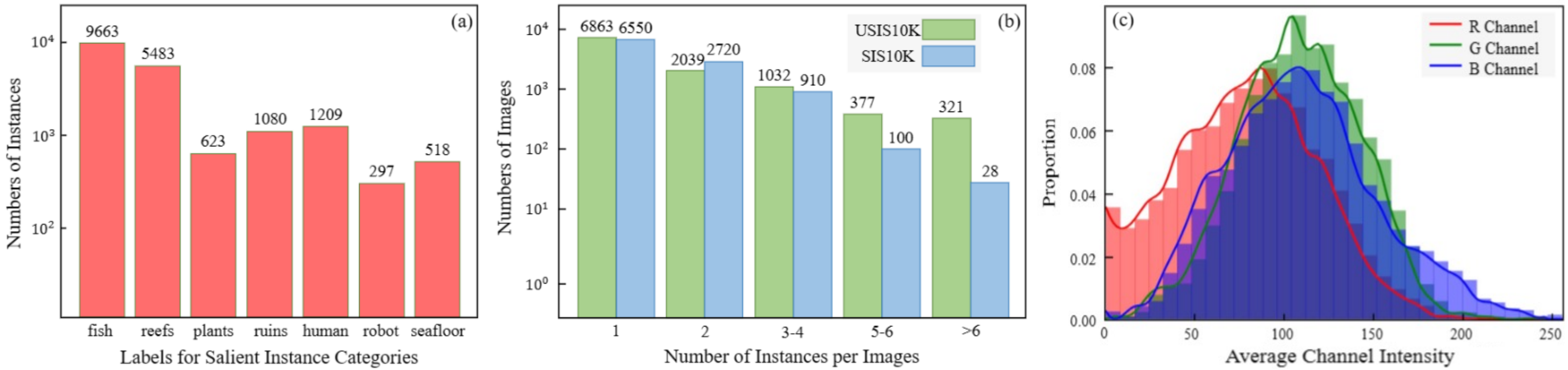

- ➢ **Challenge in the number of instance.**

  In USIS10K dataset, multiple salient instances may exist in a single image. There are 1731 images with more than 3 salient instances in our dataset, accounting for 16.3% of the total.

- ➢ **Challenges in small or large instances.**

  In USIS10K dataset, the average size of the salient instances is 34,336 pixels (approximately 185×185 pixels), which averaged 10.3% of the image size. There are 3053 salient instances smaller than 1% of the image area, (16.0% of the total), while there are 1733 instances larger than 30% of the image area, (9.1% of the total).

- ➢ **Challenges in channel intensity of underwater images.**

  Optical images inevitably suffer from color attenuation due to the selective absorption of water at different wavelengths. This poses an additional challenge for the network to properly understand and handle the image color distortion caused by this attenuation

Dataset Statistic and Challenges

- **Location of Salient Objects (Less central bias).**
  In the SIS10k dataset, approximately 13.5% of the locations have fewer than 1000 instances and 32% have fewer than 2,000 instances, while in our dataset, only 2.75% of the locations have fewer than 1,000 instances and 22.5% have fewer than 2,000 instances.

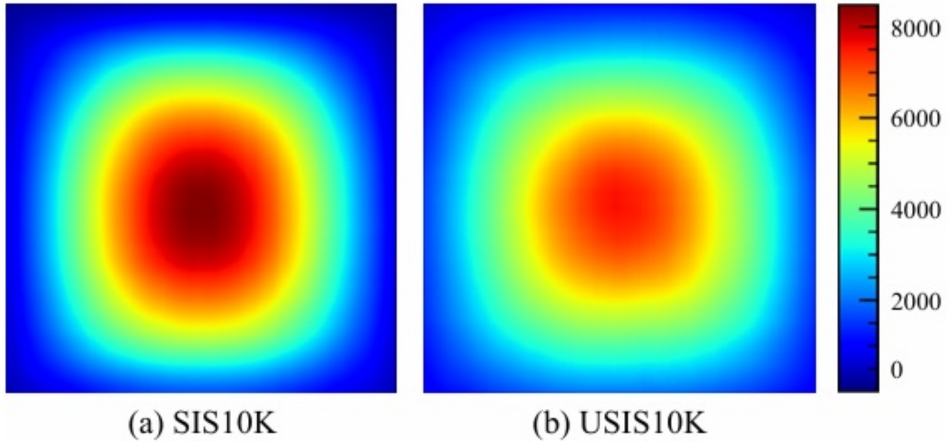

A set of salient maps from our dataset and SIS10K

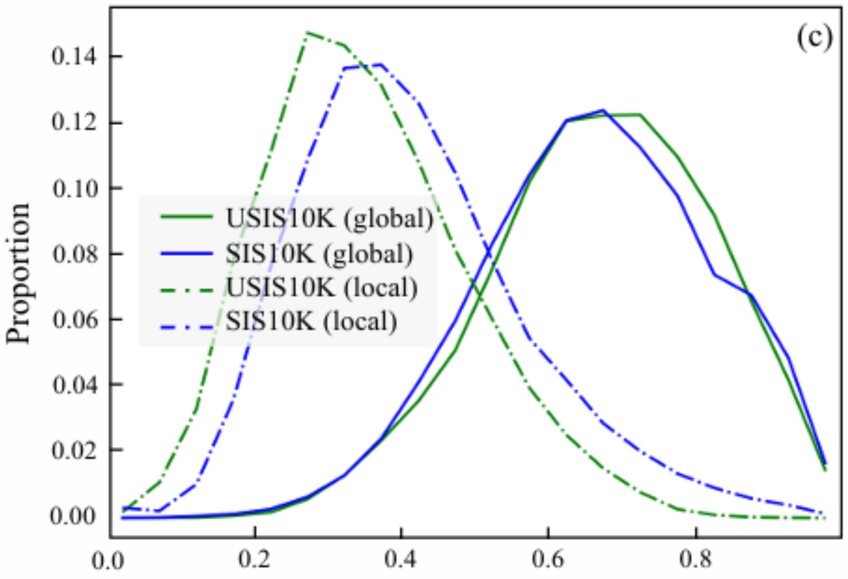

Global/Local Color Contrast of Salient Instance

- **Color Contrast of Salient Instance.**
  Saliency is often related to the contrast between foreground and background, and it is critical to check whether salient instances are easy to detect. It can be seen that the global contrast of USIS10K is slightly higher than that of SIS10K. In addition, the local contrast of USIS10K at salient instances is lower than that of SIS10K. This poses a greater challenge in accurately segmenting the salient instance masks at the network boundary portion.

USIS-SAM

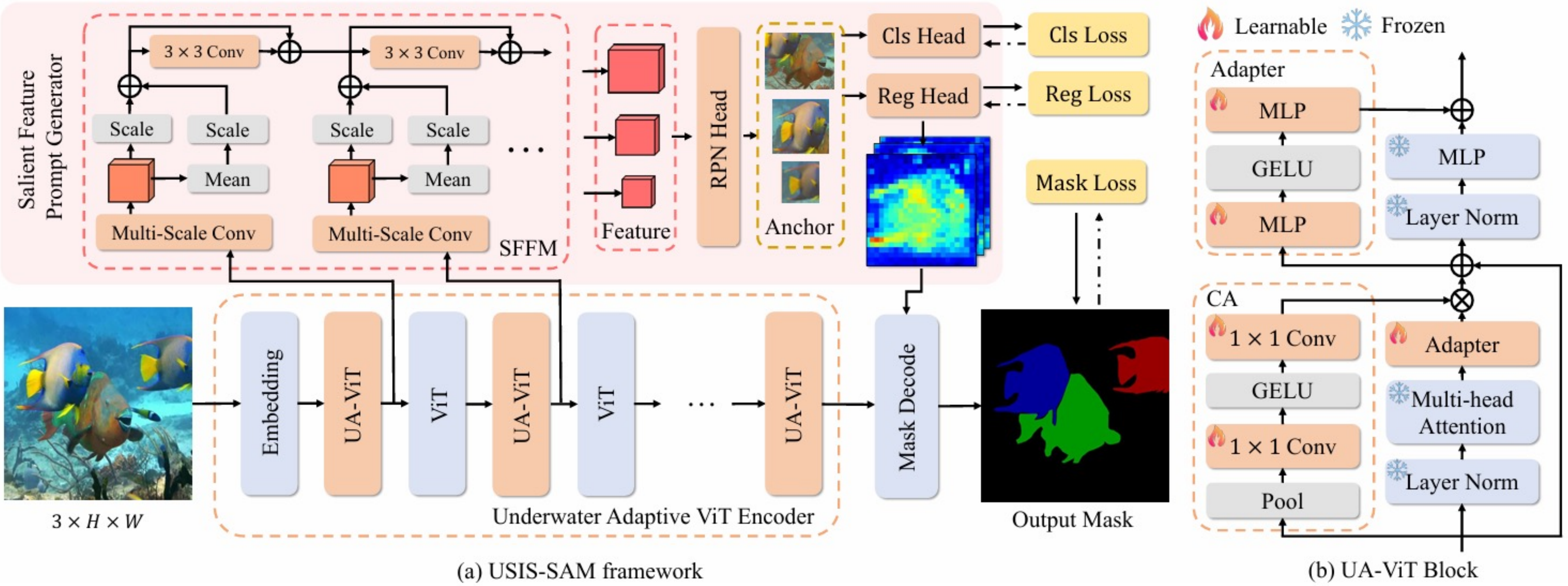

Figure 1. **(a) USIS-SAM framework.** The USIS-SAM framework modifies the SAM by adding the Underwater Adaptive ViT Encoder and the Salient Feature Prompt Generator. **(b) The structure of UA-ViT.** In the figure, SFFM stands for Salient Feature Fusion Module, CA stands for Channel Adapter.

Underwater Adaptive ViT Encoder

In USIS-SAM, we design the **Underwater Adaptive ViT (UA-ViT)** to **integrate underwater visual prompts into the network via adapter and channel adapter**. UA-ViT enables a more effective utilization of the SAM image encoder in underwater scenarios.

***Adapter*:**

$$P = MLP_{out}\,(\sigma(MLP_{prompt}(F))),$$

where F is the input feature, and P is the output prompt for each adapter layer. σ is the activation function.

***Channel Adapter*:**

$$C = F \times Conv_{up}(\sigma(Conv_{down}(Pool(F)))),$$

where C is the output feature after channel adapter, $Conv$ is a 1×1 convolutional layer, and $Pool$ is an average pooling layer.

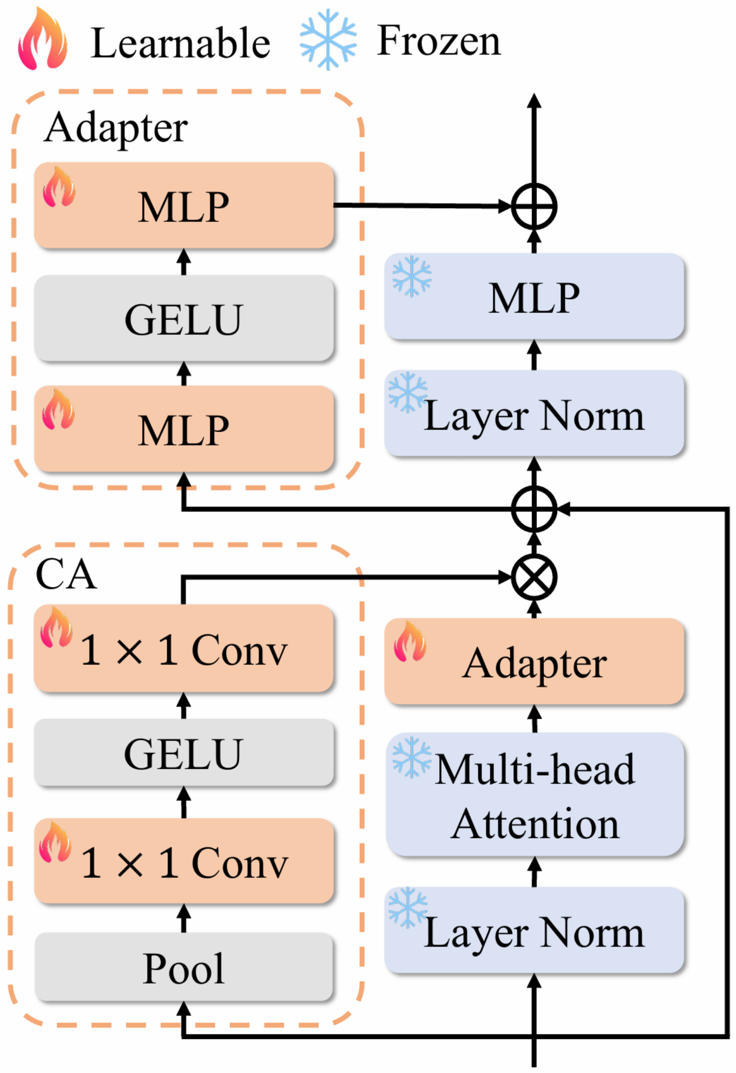

Salient Feature Prompt Generator

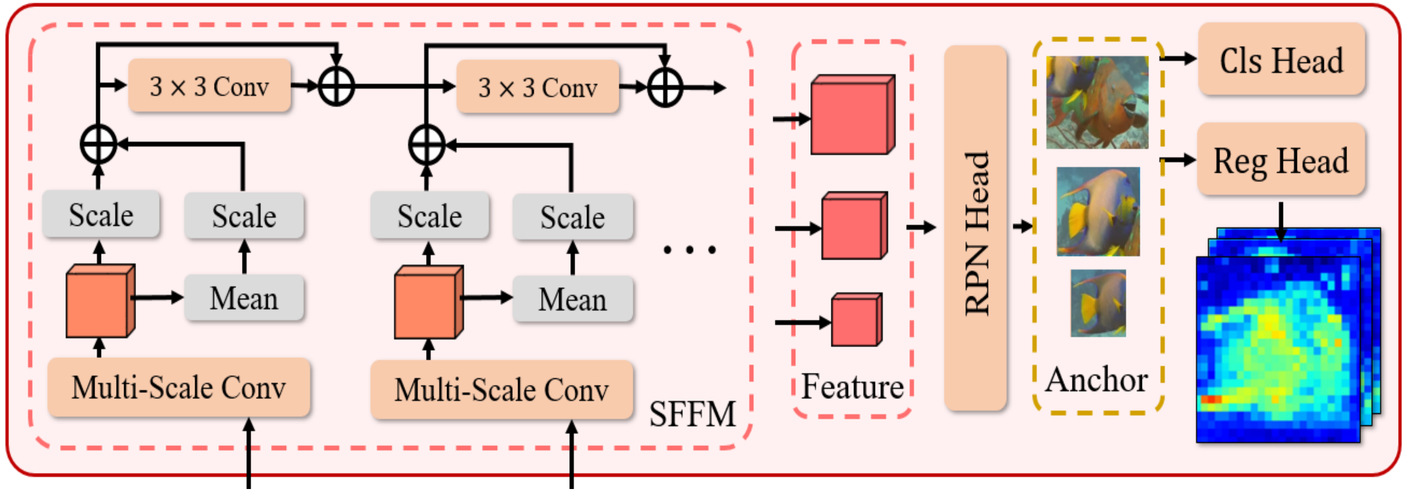

Figure 2. The structure of Salient Feature Prompt Generator (SFPG). The SFPG module efficiently filters out non-salient noise, allowing for robust feature aggregation of salient instances.

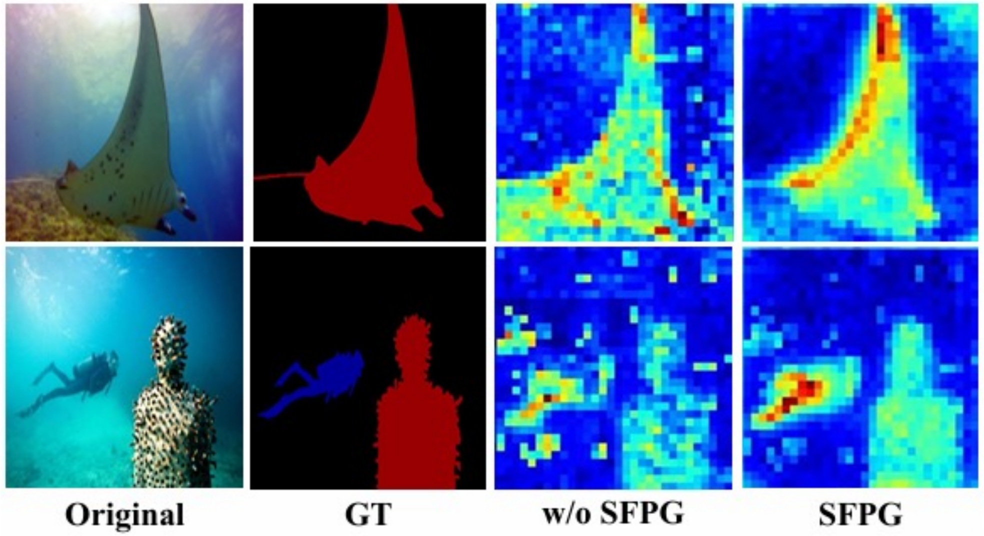

Figure 3. Visualize features generated by the Salient Feature Prompt Generator.

The USIS task needs the model to automatically recognize and segment each salient object in underwater images. However, SAM requires the user to explicitly provide foreground points, boxes, or texts as prompts to guide the model segmentation. Therefore, **we design the Salient Feature Prompt Generator to directly predict prompts embedding of salient instances, enabling end-to-end performing the USIS task**

Experiments

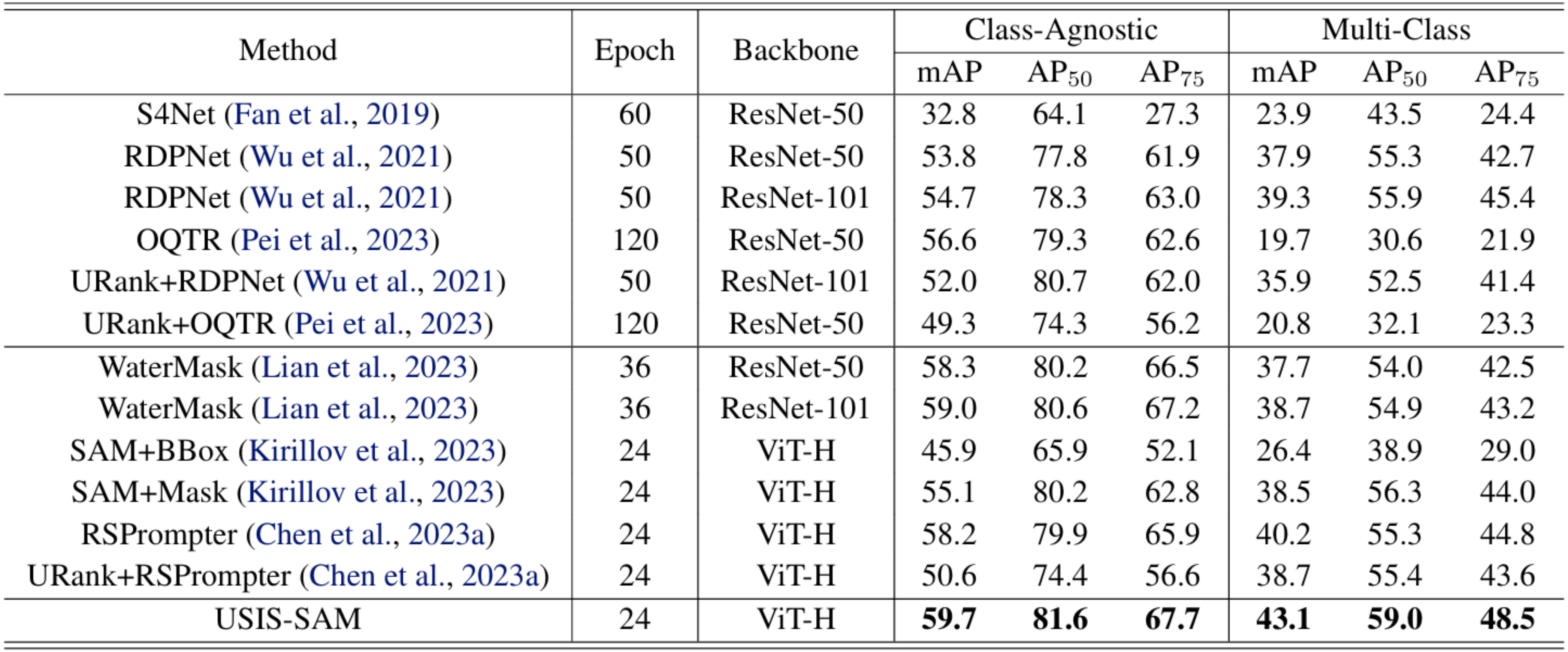

Method	Epoch	Backbone	Class-Agnostic			Multi-Class		
			mAP	AP_{50}	AP_{75}	mAP	AP_{50}	AP_{75}
S4Net (Fan et al., 2019)	60	ResNet-50	32.8	64.1	27.3	23.9	43.5	24.4
RDPNet (Wu et al., 2021)	50	ResNet-50	53.8	77.8	61.9	37.9	55.3	42.7
RDPNet (Wu et al., 2021)	50	ResNet-101	54.7	78.3	63.0	39.3	55.9	45.4
OQTR (Pei et al., 2023)	120	ResNet-50	56.6	79.3	62.6	19.7	30.6	21.9
URank+RDPNet (Wu et al., 2021)	50	ResNet-101	52.0	80.7	62.0	35.9	52.5	41.4
URank+OQTR (Pei et al., 2023)	120	ResNet-50	49.3	74.3	56.2	20.8	32.1	23.3
WaterMask (Lian et al., 2023)	36	ResNet-50	58.3	80.2	66.5	37.7	54.0	42.5
WaterMask (Lian et al., 2023)	36	ResNet-101	59.0	80.6	67.2	38.7	54.9	43.2
SAM+BBox (Kirillov et al., 2023)	24	ViT-H	45.9	65.9	52.1	26.4	38.9	29.0
SAM+Mask (Kirillov et al., 2023)	24	ViT-H	55.1	80.2	62.8	38.5	56.3	44.0
RSPrompter (Chen et al., 2023a)	24	ViT-H	58.2	79.9	65.9	40.2	55.3	44.8
URank+RSPrompter (Chen et al., 2023a)	24	ViT-H	50.6	74.4	56.6	38.7	55.4	43.6
USIS-SAM	24	ViT-H	**59.7**	**81.6**	**67.7**	**43.1**	**59.0**	**48.5**

***Table 1*. Quantitative comparisons with state-of-the-arts on the USIS10K datasets.** Urank stands for an underwater image enhancement method in UnderwaterRanker (AAAI 2023 oral), SAM+BBox uses inference results from Faster RCNN as prompts for prediction, SAM+Mask stands for Mask RCNN networks use SAM as backbone. The RSPrompter in the table is the RSPrompter-anchor framework.

Experiments

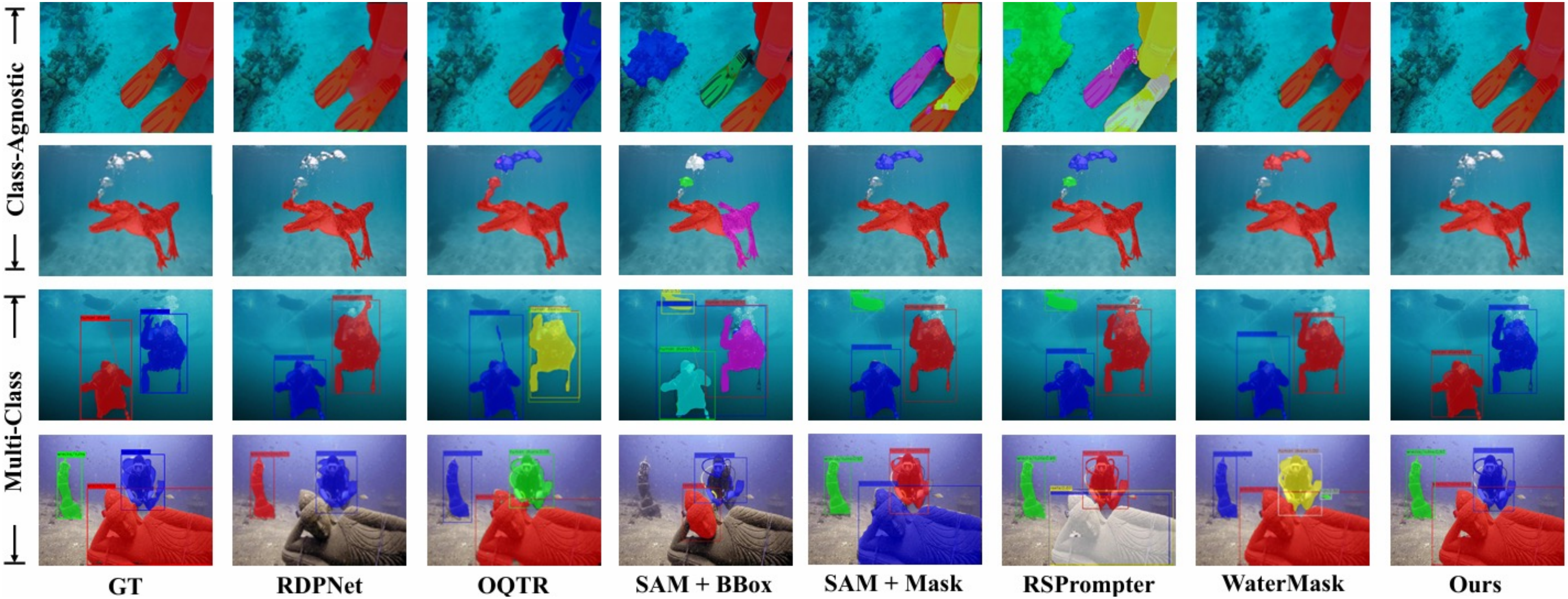

Figure 4. **Qualitative comparison on the USIS10K dataset.** Each salient instance is represented by a unique color, and the segmented mask is superimposed on the image.

Ablation Study

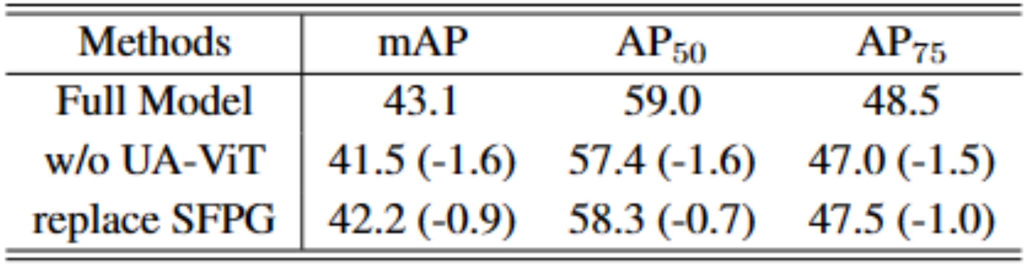

Methods	mAP	AP_{50}	AP_{75}
Full Model	43.1	59.0	48.5
w/o UA-ViT	41.5 (-1.6)	57.4 (-1.6)	47.0 (-1.5)
replace SFPG	42.2 (-0.9)	58.3 (-0.7)	47.5 (-1.0)

Table 2. Effectiveness of each component in USIS-SAM, replace SFPG means to use Multi-scale Feature Enhancer Module in RSPrompter (TGARS'24) instead of SFPG.

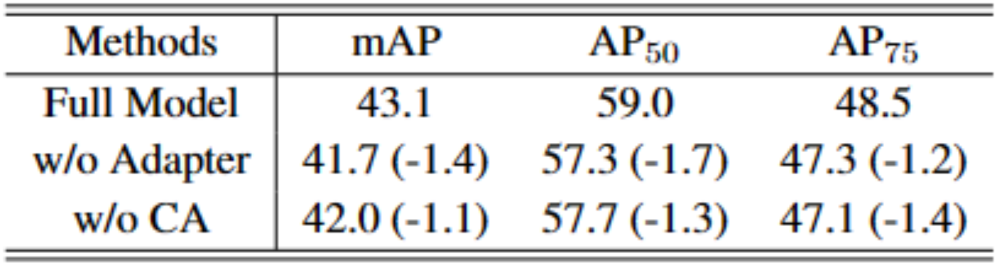

Methods	mAP	AP_{50}	AP_{75}
Full Model	43.1	59.0	48.5
w/o Adapter	41.7 (-1.4)	57.3 (-1.7)	47.3 (-1.2)
w/o CA	42.0 (-1.1)	57.7 (-1.3)	47.1 (-1.4)

Table 4. Effectiveness of each component in Underwater Adaptive ViT Encoder, w/o Adapter and w/o CA denote the removal of Adapters and Channel Adapter.

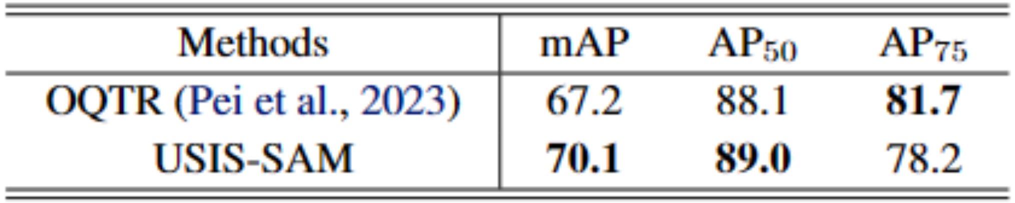

Methods	mAP	AP_{50}	AP_{75}
OQTR (Pei et al., 2023)	67.2	88.1	**81.7**
USIS-SAM	**70.1**	**89.0**	78.2

Table 3. Generalization Ability of USIS-SAM. Quantitative comparisons with state-of-the-art methods on SIS10K indicate that USIS-SAM did not overfit our dataset.

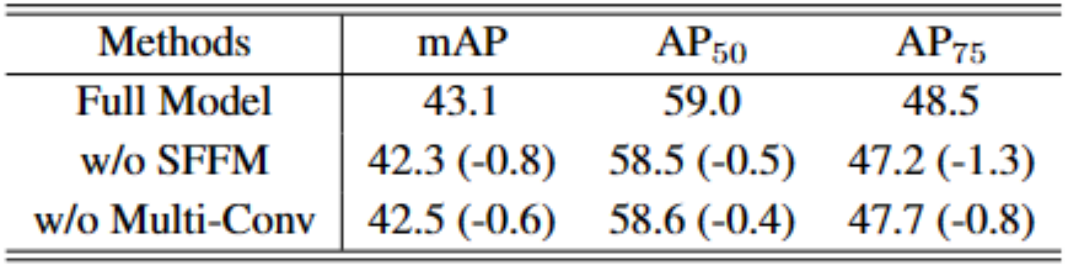

Methods	mAP	AP_{50}	AP_{75}
Full Model	43.1	59.0	48.5
w/o SFFM	42.3 (-0.8)	58.5 (-0.5)	47.2 (-1.3)
w/o Multi-Conv	42.5 (-0.6)	58.6 (-0.4)	47.7 (-0.8)

Table 5. Effectiveness of each component in Salient Feature Prompt Generator, w/o SFFM and w/o Multi-Conv denote the removal of the salient feature fusion module and multi-scale convolution module.

Conclusion and Future Work

- We have constructed the **first general underwater salient image instance segmentation dataset** with pixel-level annotations, which enables us to **comprehensively explore the underwater salient instance segmentation task**.
- we first attempt to apply Segment Anything (SAM) model to underwater salient instance segmentation and propose **USIS-SAM**, aiming to improve the segmentation accuracy in complex underwater scenes. Extensive experiments have validated the **effectiveness** and **generalizability** of USIS-SAM.
- In future work, we plan to extend the USIS datasets to **broader and more challenging underwater images and underwater videos**.

Future work

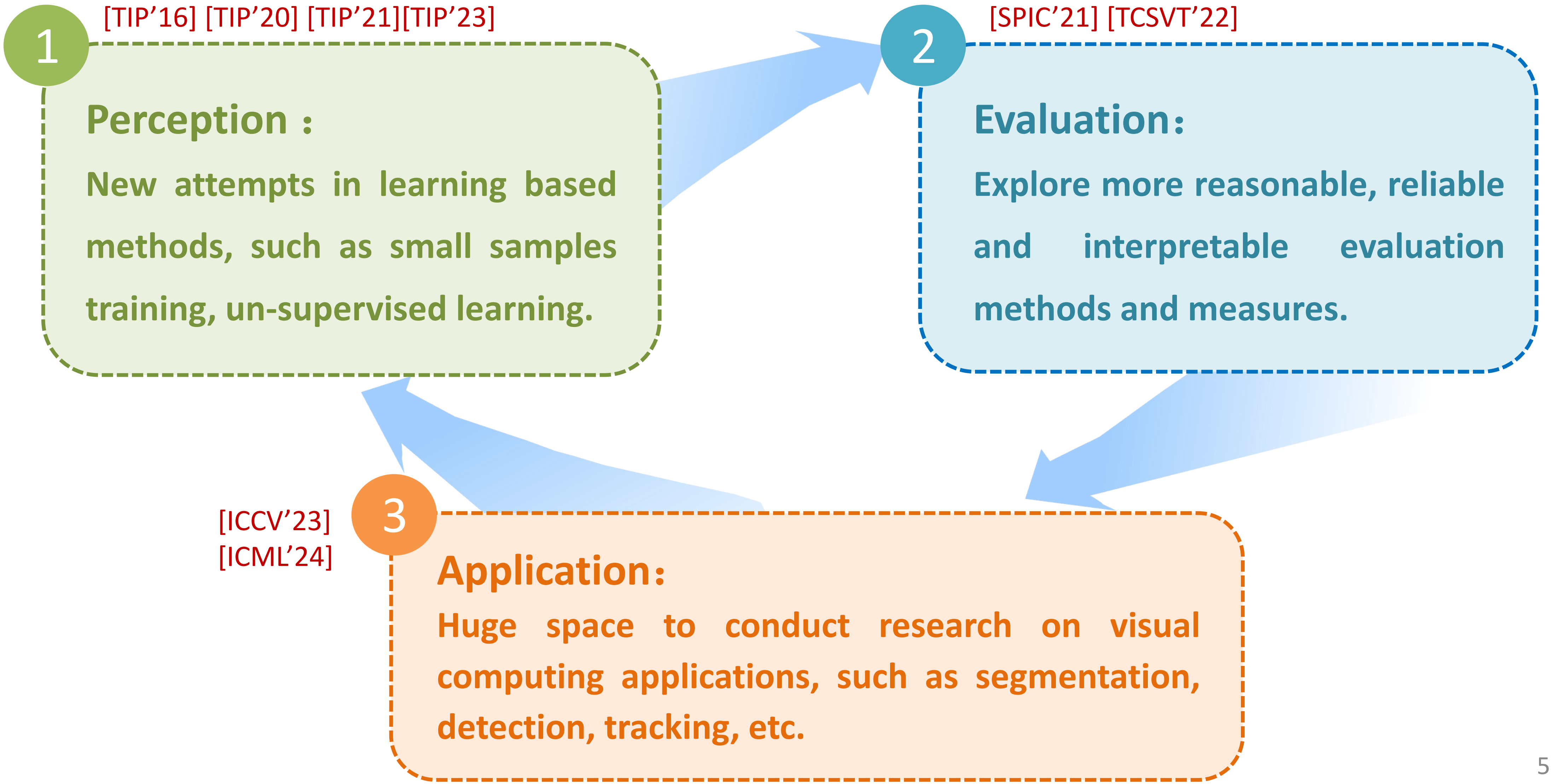

1 [TIP’16] [TIP’20] [TIP’21][TIP’23]

Perception：

New attempts in learning based methods, such as small samples training, un-supervised learning.

2 [SPIC’21] [TCSVT’22]

Evaluation：

Explore more reasonable, reliable and interpretable evaluation methods and measures.

3 [ICCV’23] [ICML’24]

Application：

Huge space to conduct research on visual computing applications, such as segmentation, detection, tracking, etc.

VSISLAB

机器智能与系统控制教育部重点实验室

Key Laboratory of Machine Intelligence & System Control, Ministry of Education

视觉感知与智能系统实验室成立于2013年9月，依托控制科学与工程国家A类学科，致力致力于智能系统感知、决策与应用领域的研究，团队包括国家级特聘教授1人、国家四青人才4人、泰山学者6人、山东省杰青3人、中国科协青托1人。目前承担国家、省部级各类科研经费3000余万元，获得国内外学术奖励10余次。

张 伟

长江学者特聘教授

控制学院副院长

宋然 教授/博导
青年拔尖

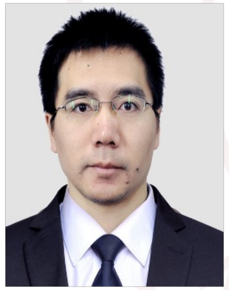

元辉 教授/博导
国家优青

丛润民 教授/博导
青年长江

张敬林 教授/博导
青年泰山

李帅 教授/博导
齐鲁青年学者

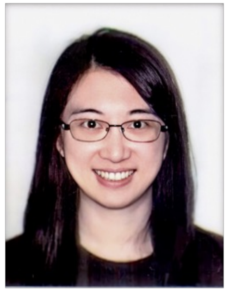

贾潇 研究员/硕导
青年泰山

香港科學會
Hong Kong Institution of Science

This is to certify that

Wei ZHANG

is a finalist to the

2010 Young Scientist Award

in

Engineering Science

Prof. C.F. NG
President
Hong Kong Institution of Science

November 2010

The 2014 IEEE International Conference on Information and Automation
& 2014 IEEE International Conference on Automation and Logistics

IEEE

2014 IEEE International Conference on Information and Automation
In conjunction with
2014 IEEE International Conference on Automation and Logistics
July 26-28, 2014, Hailar, China

Best Conference Paper

Wi-Fi Positioning Based on Deep Learning

Wei Zhang, Kan Liu, Weidong Zhang and Youmei Zhang

XU Guoqing, ICIA General Chair; FU Xi, ICAL General Chair; WU Xinyu, ICIA Program Chair; ZHU Xiangyang, ICAL Program Chair; MENG Q.-H. Max, ICIA Organizing Chair; ZHAO Jie, ICAL Organizing Chair

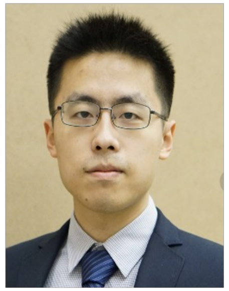

李腾 研究员/硕导
山东省优青

李晓磊 副教授/硕导
加州伯克利分校 博后

李振华 副教授/硕导
卡尔加里大学 博后

鲁威志 副教授/硕导
法国国立科学院 博士

程吉禹 副教授/硕导
香港中文大学 博士

Pourya 副教授/硕导
上海交通大学 博士

THANKS FOR WATCHING

李华 副教授

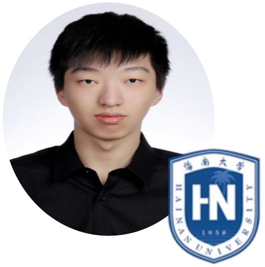
连仕杰 学士

杨文玉 硕士

Sam Kwong 教授（香港工程科学院院士）